OAK RIDGE
NATIONAL LABORATORY
MANAGED BY UT-BATTELLE
FOR THE DEPARTMENT OF ENERGY

ORNL/TM-2003/130

Cooperative Research and Development Agreement Final Report for Cooperative Research and Development Agreement Number ORNL99-0544

INTERFACIAL PROPERTIES OF ELECTRON BEAM CURED COMPOSITES

UT-BATTELLE
ORNL-27 (4-00)

ORNL/TM-2003/130

Metals and Ceramics Division

Cooperative Research and Development Agreement Final Report for Cooperative Research and Development Agreement Number ORNL99-0544

INTERFACIAL PROPERTIES OF ELECTRON BEAM CURED COMPOSITES

C. C. Eberle and C. J. Janke
Oak Ridge National Laboratory, Oak Ridge, TN 37831

J. A. Sands
US Army Research Laboratory, Aberdeen Proving Ground, MD 21005

M. S. Wilenski
The Boeing Company, Seattle, WA 98124-2499

January 2005

Prepared by the
Oak Ridge National Laboratory
Oak Ridge, Tennessee 37831-6053
Managed by
UT-Battelle, LLC
for the
U.S. DEPARTMENT OF ENERGY
under contract DE-AC05-00OR22725

This page left blank intentionally.

TABLE OF CONTENTS

This page left blank intentionally.

LIST OF FIGURES

This page left blank intentionally.

LIST OF TABLES

This page left blank intentionally.

1. EXECUTIVE SUMMARY

Electron beam (EB) curing is a technology that promises, in certain applications, to deliver lower cost and higher performance polymer matrix composite (PMC) structures compared to conventional thermal curing processes. PMCs enhance performance by making products lighter, stronger, more durable, and less energy demanding. They are essential in weight- and performance-dominated applications. Affordable PMCs can enhance US economic prosperity and national security. US industry expects rapid implementation of electron beam cured composites in aircraft and aerospace applications as satisfactory properties are demonstrated, and implementation in lower performance applications will likely follow thereafter. In fact, at this time and partly because of discoveries made in this project, field demonstrations are underway that may result in the first fielded applications of electron beam cured composites.

Serious obstacles preventing the widespread use of electron beam cured PMCs in many applications are their relatively poor interfacial properties and resin toughness. The composite shear strength and resin toughness of electron beam cured carbon fiber reinforced epoxy composites were about 25% and 50% lower, respectively, than those of thermally cured composites of similar formulations. The essential purpose of this project was to improve the mechanical properties of electron beam cured, carbon fiber reinforced epoxy composites, with a specific focus on composite shear properties for high performance aerospace applications.

Many partners, sponsors, and subcontractors participated in this project. There were four government sponsors from three federal agencies, with the US Department of Energy (DOE) being the principal sponsor. The project was executed by Oak Ridge National Laboratory (ORNL), NASA and Department of Defense (DOD) participants, eleven private CRADA partners, and two subcontractors. A list of key project contacts is provided in Appendix A. In order to properly manage the large project team and properly address the various technical tasks, the CRADA team was organized into integrated project teams (IPT's) with each team focused on specific research areas.

Early in the project, the end user partners developed "exit criteria", recorded in Appendix B, against which the project's success was to be judged.

The project team made several important discoveries. A number of fiber coatings or treatments were developed that improved fiber-matrix adhesion by 40% or more, according to microdebond testing. The effects of dose-time and temperature-time profiles during the cure were investigated, and it was determined that fiber-matrix adhesion is relatively insensitive to the irradiation procedure, but can be elevated appreciably by thermal postcuring. Electron beam curable resin properties were improved substantially, with 80% increase in electron beam 798 resin toughness, and ~ 25% and 50% improvement, respectively, in ultimate tensile strength and ultimate tensile strain vs. earlier generation electron beam curable resins. Additionally, a new resin electron beam 800E was developed with generally good properties, and a very notable 120% improvement in transverse composite tensile strength vs. earlier generation electron beam cured carbon fiber reinforced epoxies. Chemical kinetics studies showed that reaction pathways can be affected by the irradiation parameters, although no consequential effects on material properties have been noted to date. Preliminary thermal kinetics models were developed to predict degree of cure vs. irradiation and thermal parameters. These models are continually being refined and validated.

Despite the aforementioned impressive accomplishments, the project team did not fully realize the project objectives. The best methods for improving adhesion were combined with the improved electron beam 3K resin to make prepreg and uni-directional test laminates from which composite properties could be determined. Nevertheless, only minor improvements in the composite shear strength, and moderate improvements in the transverse tensile strength, were achieved. The project team was not satisfied with the laminate quality achieved, and low quality (specifically, high void fraction) laminates will compromise the composite properties. There were several problems with the prepregging and fabrication, many of them related to the use of new fiber treatments.

There remains a compelling need to further improve the mechanical properties, especially composite shear strength, of electron beam curable polymer composites. The project team was sufficiently encouraged by the bench-scale adhesion and resin improvements, and the need is considered sufficiently great, that some of the partners are continuing to address the remaining barriers in an attempt to achieve satisfactory materials integration and scale-up and to realize the overall project objectives.

2. PROJECT OBJECTIVES

The project objectives were to:

- Confirm that fiber-resin adhesion is responsible for the observed poor shear properties;
- Determine the mechanism(s) responsible for poor adhesion between carbon fibers and epoxy resins after electron beam curing;
- Develop and evaluate resin systems and fiber treatments to improve the properties of electron beam cured, carbon-fiber-reinforced composites; and
- Develop refined methods for processing electron beam cured, carbon-fiber-reinforced composites.

3. BENEFITS TO DOE

Composite materials are beneficial to DOE for both energy efficiency and energy production missions. The high specific strength and specific stiffness of carbon fiber reinforced polymers enables beneficial mass reduction in many structures. Vehicle mass reduction decreases petroleum-based fuel demand, thereby enhancing transportation energy efficiency. Wind turbines with megawatt range power ratings typically utilize fiber reinforced composite blades. Composites also can reduce the size and cost of deepwater offshore oil platforms. Electron beam curing may offer cost and/or performance benefits in all of these composite material applications. Improving the properties of electron beam cured materials is a necessary step for its utilization in the aforementioned energy-related composite materials applications.

4. TECHNICAL DISCUSSION

4.1. Background

Electron beam curing is a technology that promises, in certain applications, to deliver lower cost and higher performance PMC structures compared to conventional thermal curing processes. PMCs enhance performance by making products lighter, stronger, more durable, and less energy demanding. They are essential in weight- and performance-dominated applications. US industry expects rapid implementation of electron beam cured composites in aircraft and aerospace applications as satisfactory properties are demonstrated, and implementation in lower performance applications will likely follow thereafter. In fact, at this time and partly because of discoveries made in this project, field demonstrations are underway that may result in the first fielded applications.

Serious obstacles preventing the widespread use of electron beam cured PMCs in many applications are their relatively poor interfacial properties and/or resin toughness. Previous research on electron beam cured carbon fiber reinforced epoxy composites has documented that interface dependent properties such as composite shear strength are about 25% lower than those of thermally cured composites of similar formulations.[1,2,3,4,5,6,7] Similar observations have been made in composite systems involving electron beam cured carbon fiber reinforced vinyl esters[8]. Furthermore, electron beam cured epoxy resin toughness tends to be just over half that of state-of-the-art thermally cured epoxies. Short beam shear (SBS) testing is an inexpensive, commonly used method for characterizing composite shear strength, and SBS strength can be compromised by either fiber-matrix adhesion or resin toughness. In fact, both were deficient in electron beam cured composites. The essential purpose of this project was to improve the mechanical property profile of electron beam cured, carbon fiber reinforced epoxy composites, with a specific focus on composite shear properties. It is expected that the principles and methods of this project can be applied to almost any electron beam cured, fiber reinforced, polymer material system.

4.2. Project Management

Many partners, sponsors, and subcontractors participated in this project. Federal government sponsors included the US Department of Energy, Office of Science, Laboratory Technology Research Program; NASA Langley Research Laboratory; US Air Force Research Laboratory; and US Army Research Laboratory. In addition to providing funding, the NASA and DOD sponsors were active technical participants in the project. CRADA partners included Acsion Industries, Adherent Technologies Inc., Applied Poleramic Inc., The Boeing Company, Cytec Industries Inc. (Amoco Performance Products when the project commenced), E-Beam Services Inc., Hexcel Corporation, Lockheed Martin Corporation, STERIS Corporation, UCB Surface Specialties (formerly UCB Chemicals Corporation), and YLA Inc. Subcontractors included Michigan State University (contract with ORNL) and the National Research Council of Canada (contract with Acsion Industries). A list of key project contacts is provided in Appendix A.

In order to properly manage the large project team and properly address the various technical tasks, the CRADA team was organized into IPT's with each team focused on specific research tasks.

- The Adhesion IPT was focused on understanding the reason for characteristic poor adhesion between the fiber and resin in electron beam cured composites, and how to improve the adhesion.
- The Irradiation IPT was focused on providing irradiation support for the other IPT's, evaluating the effects of irradiation parameters on composite properties, especially interlaminar shear and toughness, and on improving the composites community's understanding of irradiation technology.
- The Materials & Processing (M&P) IPT was focused on developing constituent materials and processing methods that produce better composite properties, especially resin toughness.
- The Kinetics IPT was focused on identifying and characterizing reaction mechanisms and kinetics that govern polymerization; understanding how reaction mechanisms and kinetics influence material properties; and determining whether changes in material formulations or processing parameters can modify reaction mechanisms and kinetics in a way that will yield improved material properties.
- The Leadership IPT consisted of the respective technical IPT leaders and project management staff. It was responsible for coordinating project activities among the technical IPT's and ensuring that all activities were designed to achieve progress toward accomplishment of the essential project objectives.

Late in the project, the adhesion and M&P groups were merged into a single group addressing materials integration.

4.3. Reference Data

The project team chose a baseline material system from which resin and composite property improvements would be measured. The baseline material system was Hexcel's unsized AS4 fiber with standard surface treatment, electron beam curable resin Tactix 123 for neat resin and single fiber studies "Cat-B" resin for laminates, and 3 phr of CD-1012 photoinitiator. Tactix 123 was chosen as the baseline resin for characterization work because it is a simple epoxy which makes a good model compound; is cheap and readily available; and can readily be filament wound. "Cat-B" was one of the better performing electron beam curable resins for which there was a reasonable amount of laminate data. The CD1012 initiator was baselined because it was commercially available and much cheaper than the alternate, it performs well in most applications, and it was deemed most likely to be the first initiator to be implemented at significant volume. Hexcel's AS4 fiber is a commonly used, relatively inexpensive aerospace grade fiber for which there exists a substantial database of composite properties. Furthermore, AS4 roundness and diameter make it amenable to single fiber indentation testing.

The project team chose not to define a formal irradiation processing baseline. Historically, cationic epoxy cure doses had been determined to range from about 100 kGy to 200 kGy, usually delivered in several increments. This was therefore the starting point for irradiation processing studies.

Early in the project, the end user partners, Boeing and Lockheed Martin, developed "exit criteria", recorded in Appendix B, against which the project's success was to be judged. The levels correspond to recommended test order, i.e., level 1 parameters can be tested quickly and inexpensively, so they comprise the most logical first tier of tests with materials passing the level 1 tests then subjected to the more expensive and time-consuming level 2 test battery. It should be noted that the exit criteria are derived from state-of-the-art, thermally cured aerospace material

properties, and therefore present challenging targets in high performance applications. The exit criteria would be expected to be considerably less demanding for lower performance, consumer-driven applications, although other demanding criteria might be added.

4.4. Adhesion

The Adhesion IPT characterized fiber-matrix adhesion in electron beam cured composites, and developed methods for improving the fiber-matrix adhesion.

4.4.1. Adhesion IPT Mission

The mission of the Adhesion IPT was to improve the adhesion of electron beam cured carbon fiber reinforced epoxy composites so that they meet or exceed their thermally cured counterparts. The researchers were to determine the source of the low adhesion in current electron beam cured systems, and use this understanding to improve their adhesion. Improvement methods should be economical, environmentally friendly, applicable to multiple resin/fiber systems, and compatible with the beneficial aspects of electron beam curing.

4.4.2. Adhesion Technical Strategy

The technical strategy for improving fiber-resin adhesion was to determine the source of the low properties in current electron beam cured systems, and to use the results to improve fiber-resin adhesion, as follows.

- Interface characterization – The fiber-resin interface was chemically and mechanically characterized in order to understand the mechanisms responsible for and the nature of the adhesion deficiency.
    - Baseline database – Adhesion data was compiled for selected thermally cured systems as well as the incoming electron beam curable systems. The electron beam cured systems were shown to be deficient in off-axis and toughness properties.
    - Fiber surface chemistry – The extent of adsorption and deactivation of the carbon fiber surface chemistry under irradiation was determined using tools such as XPS, DSC, and chemisorption studies. The electron beam does not appear to change the fiber surface during irradiation.
    - Fiber-resin adhesion – Fiber-resin adhesion has been characterized via single fiber compression tests and found to be deficient for the baseline systems.
- Interface modification – The fiber-resin interface was re-engineered by one or more of the following techniques to resolve the adhesion deficiency.
    - Fiber surface treatments – Fiber surface treatments were specifically designed for promoting adhesion to electron beam curable epoxy resins. Fiber surface treatments involve a chemical modification of the nascent fiber surface that alters the surface chemical composition, such as oxidation, acid-base reactions, and etching, without a deliberate coating of the surface. A plasma treatment was shown to successfully increase adhesion.
    - Fiber coatings – Fiber coatings, including coupling agents, reactive finishes, and sizings, were designed for use with electron beam cured resins. Each of these coating techniques showed some success.
    - Resin – The resin parameters that are most likely to affect adhesion were systematically investigated. The surface energy was found to be important, and thus the use of a surfactant in future resin compositions is recommended if the surface en-

ergy is too high. An increase in resin tensile strength was found to be needed. The resins were found to be deficient in toughness as well, though no direct relationship between this property and adhesion was investigated.

4.4.3. Adhesion Technical Accomplishments

4.4.3.1. Understanding the Problem

The transverse tensile strength of the electron beam cured graphite epoxy composite IM7/3K is only 45% of the transverse tensile strength of several successful thermally cured graphite epoxies with resins having fracture toughness similar to 3K. This result is consistent with data in the literature indicating reduced off-axis properties in electron beam cured composites. Resin tensile strength, resin cure shrinkage, and interfacial tensile strength were identified for further development that may improve the transverse strength of IM7/3K and the off-axis properties of electron beam cured composites in general. The tensile strength of 3K (and several other electron beam curable resins) should be a primary candidate for research since it was 30% lower than the tensile strength of thermally cured resins with equivalent fracture toughness. However, calculations based on resin and composite mechanical test results indicate that even if the tensile strength of 3K were made equivalent to the baseline thermal cure resins, the transverse strength of IM7/3K would not reach the composite transverse strength of the thermal cure composites. Therefore, the adhesion between the fiber and matrix is *the factor limiting* the transverse strength of IM7/3K. This is supported by "cruciform" testing which showed interfacial failure prior to resin failure for electron beam cured samples, while baseline thermally cured samples showed macroscopic resin failure prior to disbond. Increased resin cure shrinkage, although a source of residual stresses and dimensional instabilities in laminates, is also a viable method of achieving incremental improvements in composite transverse strength since interfacial debonding would be delayed[9].

4.4.3.2. Adhesion Findings

A number of important conclusions can be drawn from the adhesion research performed during this project. For ease of reading, they have been broken into areas by topic. Supporting data can be found in the publications listed in section 5.2 of this report.

The most important conclusions of this research project are:

As far as the matrix is concerned…

- Curing is very fast,
- Temperature profile/dose increments influence curing kinetics,
- Cations can be trapped into the material,
- Particles of initiator residues can be found in the resin,
- Current electron beam cured matrices have lower properties than corresponding thermally cured matrices.

As far as adhesion is concerned…

- Adhesion is highly related to the bulk matrix properties,
- Dose and dose increments do not directly influence the adhesion,

- Adhesion is higher for undercured material,
- Surfactants that reduce the resin surface tension aid in adhesion.

As far as thermal postcuring is concerned…

- Postcuring increases adhesion of fully cured material,
- Chemical bonding occurs between the matrix and the fibers upon heating,
- Postcuring can degrade the material properties,
- Cationic species trapped into the material evolve upon heating (postulated to be degradation of ionic bonding),
- Particles evolve into the resin upon postcuring.

As far as new surface treatments and sizings are concerned…

- Sol-Gel sizings can improve adhesion
- Isocyanate sizings can improve adhesion
- Plasma treatment can be very efficient to increase adhesion in carbon fiber reinforced epoxy composites (+90%),
- Epoxy-novolac sizings have a limited efficiency to increase adhesion,
- Dialdehyde sizings can also increase adhesion to carbon fibers (45%),
- Epoxy sizing with high photoinitiator concentration can significantly increase adhesion.

Interfacial Improvement Candidates

Based on microdebond testing, the candidates shown in Table 1 were chosen for scale-up testing.

Table 1. Best adhesion improvement candidates

Adhesion Solution	Adhesion Improvement	Principal Developer
Hexcel R-Sizing	40%	Hexcel Corporation
Sol-Gel	20-50%	The Boeing Company
Plasma treatment	40-90%	Michigan State University (scale-up by Adherent Technologies)
Isocyanate	50%	UCB Chemicals
High Initiator Concentration	25-90%	Oak Ridge National Labs

4.4.4. Adhesion Conclusions

The Adhesion IPT generated a large amount of data and is well on the way to understanding both the problem and solution to the low properties in electron beam cured composites. A 25% increase in transverse tension was achieved using a sol-gel to bond to active sites on the fiber and provide epoxide groups for reaction into the matrix resin. A 10% increase was achieved due to simple fiber surface modification using plasma treatment. Further isocyanate testing was inconclusive, largely because of the difficulty of making enough sizing to fabricate and test laminates on a reasonable scale.

Based on the knowledge that the resins are also deficient, it is highly likely that a combination of the improved performance resin developed by the M&P IPT and the adhesion im-

provements seen here may cause the dramatic property improvement desired. Further tests are planned to combine these improvements.

4.5. Materials & Processing

The Materials & Processing IPT made significant progress toward developing electron beam curable cationic epoxy resins having improved fracture toughness and tensile properties and improved composite transverse tensile strengths with better fiber pull-out, as well as a clearer understanding of the variables affecting void content in electron beam cured laminates.

4.5.1. Materials & Processing IPT Mission

The mission of the Materials & Processing IPT was to develop improved electron beam curable epoxy resin systems and processing methods for producing electron beam cured composites that meet or exceed the thermo-mechanical properties of autoclave cured, carbon fiber reinforced composites containing Cytec's toughened epoxy resins 977-2 or 977-3, or Hexcel's untoughened 3501-6 epoxy (interim target). To achieve this goal particular emphasis was placed on overcoming limitations of neat resin toughness, neat resin tensile properties, and composite transverse tensile strength without impairing modulus, thermal stability, or processibility, and also to develop a better understanding of the critical variables that affect the void content when fabricating electron beam cured composite laminates.

4.5.2. Materials & Processing Technical Strategy

The technical strategy for the Materials & Processing IPT was to improve the neat resin toughness, neat resin tensile properties, and composite transverse tensile strength while maintaining balance of properties, and to better understand the critical variables for minimizing laminate void content. This strategy included the following:

- Enhanced cationic epoxy neat resin toughening, neat resin tensile properties (strength, modulus, strain-to-failure), and improved composite transverse tensile strengths were attempted by changing the resin backbone via chain extension agents or co-reactants, and/or by the incorporation of various toughening materials and/or by modifying radiation cure parameters. Typical methods that are currently used to toughen thermally curable epoxy resins including the incorporation of acrylonitrile containing rubber materials (i.e. CTBN or ATBN rubbers) or adding high percentages (>10-15%) of thermoplastics are not applicable for toughening electron beam curable cationic epoxy resins due to cure inhibition and processing limitations (i.e. exceedingly high resin viscosities, incompatible phase separation kinetics), respectively.
  - Baseline database – Data on neat resin fracture toughness, neat resin tensile properties, and composite transverse tensile strength was compiled for selected, state-of-the art thermally cured resin systems as well as incumbent electron beam curable resin systems. Incumbent electron beam cured resin systems have been shown to be adequate in terms of neat resin tensile modulus and glass transition temperature, however, these systems are deficient in neat resin toughness, neat resin tensile strength, neat resin tensile strain-to-failure, and composite transverse tensile strength.
  - Neat resin fracture toughness, neat resin tensile properties, and composite transverse tensile strength of newly developed electron beam cured toughened resins were determined,

using applicable ASTM testing criteria, and compared with selected, state-of-the art thermally cured resin systems and incumbent electron beam curable resin systems.

- Promising electron beam curable, toughened resin candidates were prepregged with AS4 carbon fiber, laid-up and electron beam cured into composite laminates, then mechanically tested. The tests included short beam shear strength, flexural strength, flexural modulus, composite transverse tensile strength, void content, C-scan, and fiber pullout. Final resin down-selection was conducted in coordination with the Adhesion IPT. Some of the important processing attributes included in the resin down-selection process included resin viscosity profiles, prepreg process sensitivity, ease of laminate lay-up and cure, and level of laminate consolidation.

- A parametric study was conducted to understand the critical variables that affect the void content in electron beam cured laminates. Parameters investigated include: resin type (toughened vs. untoughened); debulk temperature (room temperature vs. elevated); debulk time (minutes vs. hours); debulk frequency (number of plies laid down before debulk); additional external pressure applied during debulk; additional debulking applied at irradiation site; resin bleed vs. non-bleed during debulk; bleed-out materials sequence (slow bleed vs. fast bleed); delayed cure (weeks vs. immediate cure after debulk); laminate area; laminate thickness; layup operator; electron beam dose increment (5-50 kGy/pass); laminate location sampled for composition (edge vs. center). Voids were found to be generally on the interface between plies in all cases. This indicates that air trapped during lay-up was not being allowed to escape rather than volatiles produced during cure being the problem. Open architecture prepregs may be a route that could be investigated in follow-on studies to help eliminate the trapped air.

4.5.3. Materials & Processing Technical Accomplishments

A variety of approaches were used for improving the toughness of electron beam curable cationic epoxy resin systems. These toughening strategies included chain extension of the epoxy resin backbone; high epoxide equivalent weight resins; flexible epoxy resins; single phase and/or 2nd phase thermoplastic resins; inorganic particles; core shell materials and rubbers; dendritic hyperbranched polymers; acrylate resins; and uniquely shaped epoxy resins.

Several toughened resins have been developed having improved properties including glass transition temperatures and tensile moduli that are comparable to those of several state-of-the art thermally cured (177°C) epoxy resin systems. These electron beam cured resins have minimum glass transition temperatures of 177°C, tan delta (dynamic mechanical analysis), and 173°C, peak loss modulus, and tensile moduli of 0.5 - 0.6 Msi versus 0.5 - 0.7 Msi for thermally cured materials.

Significant improvements in neat resin toughness (K_{IC}) were attained for a number of newly developed electron beam curable resins. In particular, electron beam Resin 798 met the CRADA target value and exhibited an 80% improvement in K_{IC}, and is comparable in toughness to some of the toughest thermally cured epoxies, as shown in Figure 1.[10, 11]

A 25% increase in neat resin tensile strength was also realized with these new resins compared to earlier electron beam resins, with electron beam Resins 798 and 800E being comparable to most thermally cured epoxies, as shown in Figure 2.[9, 10, 12]

In addition, a 50% improvement in resin tensile strain-to-failure was attained versus earlier electron beam epoxies, with electron beam Resins 798 and 800E having comparable values to Cytec's 977-2 toughened epoxy, and exceeding several other thermally cured epoxy resins, as shown in Figure 3.[9, 10, 12]

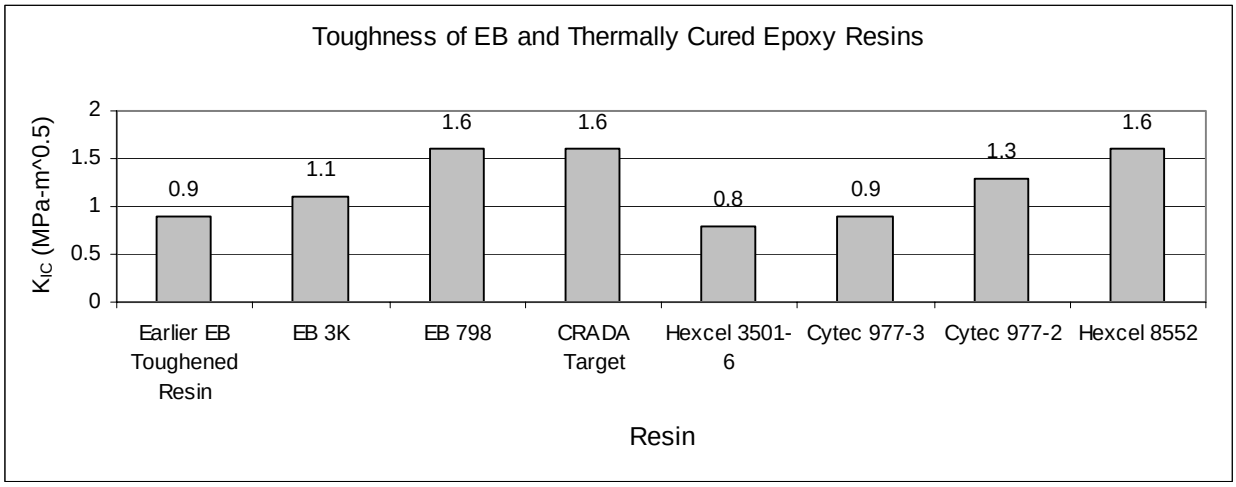

Figure 1. Mode I fracture toughness of various resins.

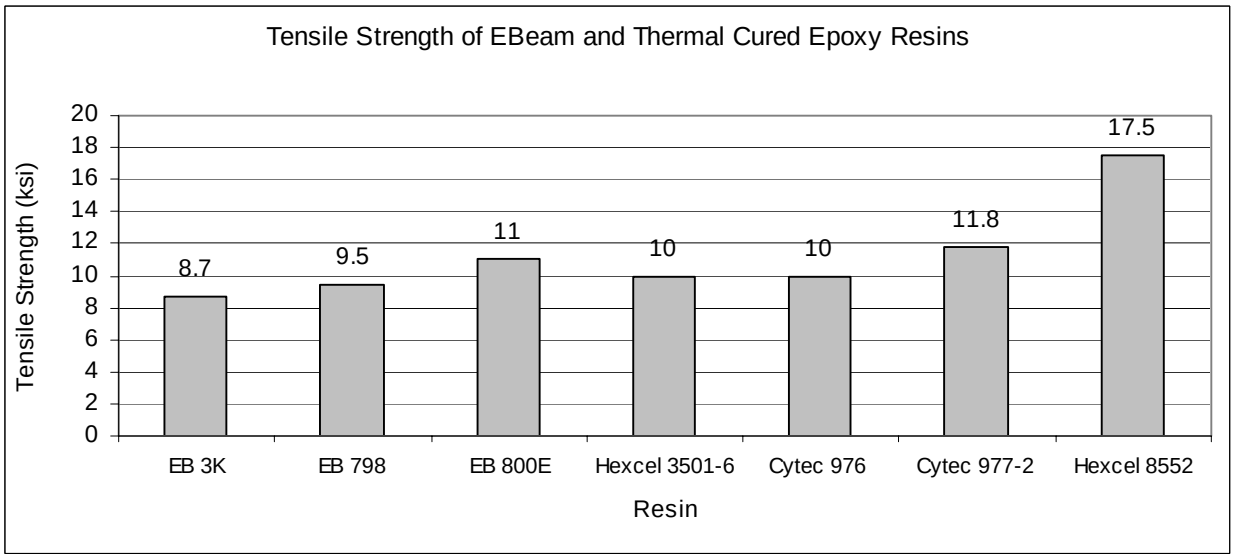

Figure 2. Ultimate tensile strength of various resins.

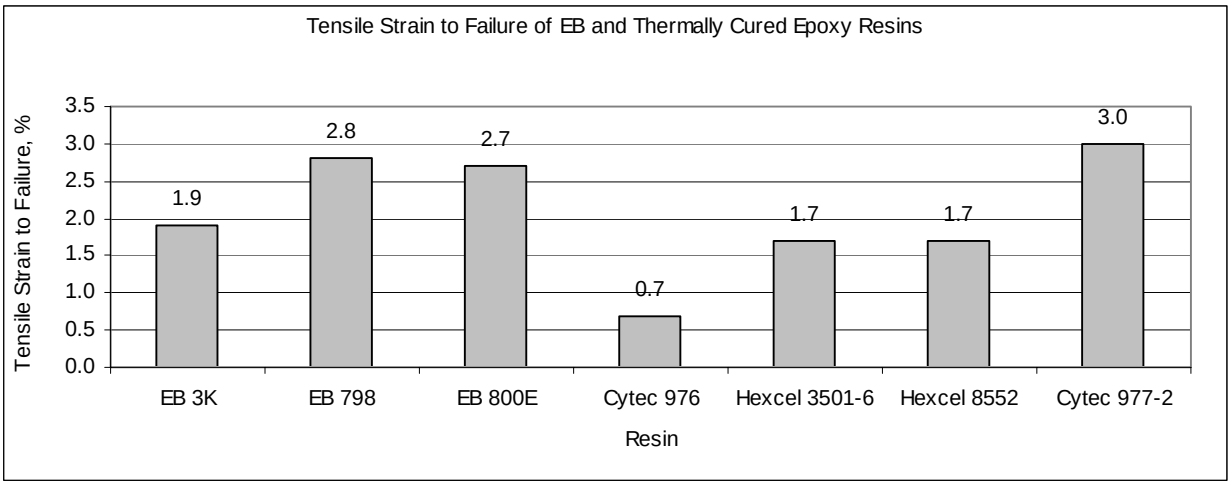

Figure 3. Tensile strain-to-failure of various resins.

In terms of laminate properties, electron beam Resin 800E exhibited a 120% improvement in composite transverse tensile strength compared to earlier carbon fiber reinforced electron beam composites, and is comparable to most thermally cured composites and this material also met the CRADA target value, as shown in Figure 4.[9]

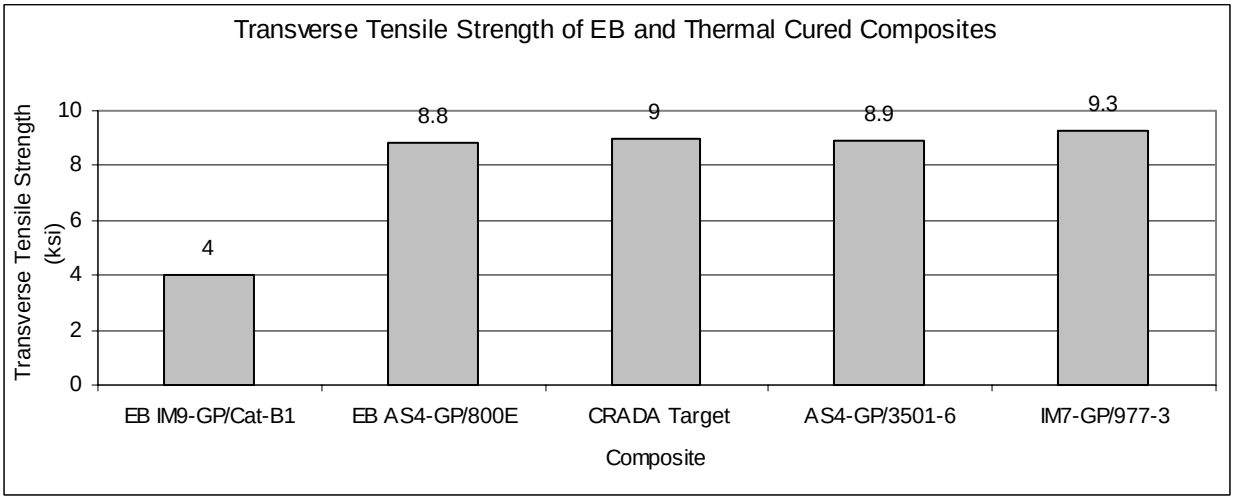

Figure 4. Transverse tensile strength of various resins.

The electron beam cured, AS4/800E composite also demonstrated greatly improved fiber pullout compared to all other electron beam cured composites, indicating higher fiber matrix adhesion, as shown in Figure 5 and discussed in Table 3.[11]

However, the AS4/800E composite fabricated with conventional GP fiber sizing did not exhibit an interlaminar shear strength any higher than most electron beam cured composites. Since all laminates in the scale-up studies had greater void content than the thermally cured baselines and the voids were on the interlaminar planes between plies, and the void contents were greatest on the interlaminar mid-plane of the laminates (where the failure occurs in SBS)

the SBS properties are likely not representative (i.e. lower) than the shear strengths that could be achieved in the absence of voids. Various properties of AS4 carbon fiber reinforced composites incorporated with the newly developed, down-selected electron beam cured resins are listed in Table 2. For most of these laminates the void contents were very encouraging with most values well under 1%.

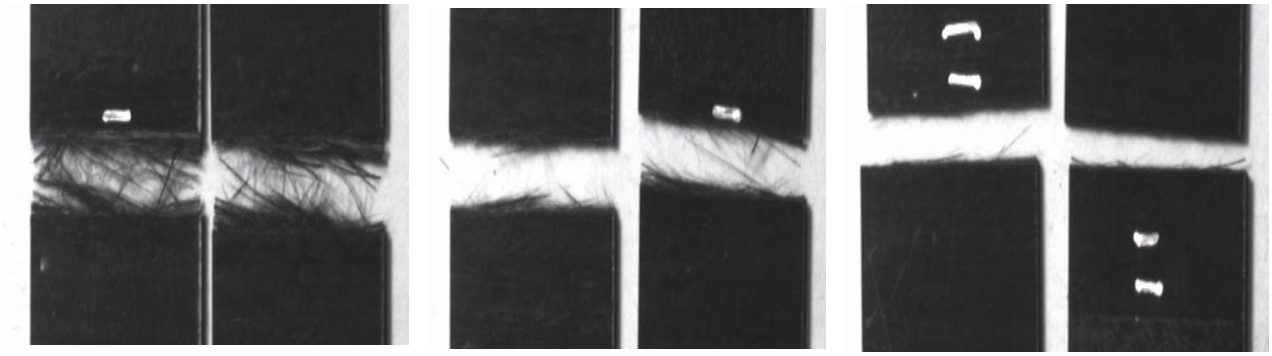

101 Resin- High 3K Resin – Medium 800E Resin–Low-medium

Figure 5. AS4 fiber pullout results.

Table 2. Data from fabrication parametric study

Panel #	Resin	Sizing	Comp. Transverse Strength (ksi)	SBS Strength (ksi)	Thickness (in.)	Fiber pullout (see Figure 5)	Void Content (%)	NDI	Viscosity	Matrix KIC (MPa m1/2)	Matrix tens. str. (ksi)
1	74A	R	2.55	11.56	0.088	Extreme	0.02	147.8	6000		
2	50D	GP	5.56	12.27	0.091	Moderate	0.18	147.8	7600		
3	101	GP	3.63	9.45	0.081	Extreme	3.62	136.9	2000		
4	1200	GP	3.93	9.8	0.086	Extreme	0.86	140	2400		
5	800E	GP	8.79	10.69	0.085	Low/Mod.	0	148.8	4400	0.7	11
6	3KM	GP	6.86	11.67	0.085	Moderate	0.34	147.4	4500		
7	3K	GP	6.62	12.21	0.084	Moderate	0.07	150.3	5000	1.1	8.7
8	798	R or GP?	3.08	7.3	0.079	Extreme	0.16	134.4	1800	1.6	9.5
9	798	R or GP?	4.67	7.47	0.082	Extreme	2.5	123.8	1800	1.6	9.5
IM7/977-3		GP	9.3 - 9.6	18-19		Low to zero	<0.05			0.9	11.9
AS4/3501-6		GP	8.9	18-19		Low to zero	<0.05			0.9	12.5
IM7/5250-4		GP	10	20		Low to zero	<0.05			0.9	12.5

Results from the parametric study that focused on understanding the critical variables for reducing void content in electron beam cured laminates provided some useful information for fabricating better consolidated composites.[13] The findings included the following:

- The single factor that consistently produced the lowest voids in electron beam cured laminates was elevated temperature debulking, applied at regular intervals during lay-up; For example, the void fraction in 24-ply, electron beam cured AS4/3K laminates were reduced from 2-4% to 1-2% by debulking at 70°C after every 4 plies. Debulking AS4/3K laminates at 100°C produced void content < 1%.

- Room temperature debulking reduces void content, but less effectively than elevated temperature debulking.
- Lower temperature debulking can also be effective in reducing laminate void content, provided debulking time is increased.

4.5.4. Conclusions

The M&P IPT developed and evaluated new toughened electron beam curable epoxy resins with a few of them possessing encouraging properties. In comparison to earlier generation electron beam resins, an 80% improvement in resin toughness was achieved with electron beam Resin 798, and electron beam Resin 800E exhibited a 25% improvement in resin tensile strength, a 50% improvement in resin tensile strain-to-failure, a 120% improvement in composite transverse tensile strength, and has improved fiber pullout. In addition, the M&P IPT has developed a clearer understanding of the critical parameters affecting laminate void content.

4.6. Materials Integration

After the development of improved resins and several promising adhesion promoting solutions, the project team began to address integration of the various project aspects to produce a competent material system. An experimental matrix was developed that included:

- Various adhesion promoting solutions prepregged with either Hexcel's AS4 12K fiber or Cytec's T-300/12K fiber with electron beam 3K resin;
- Various resins prepregged onto Hexcel's AS4-GP 12K fiber with GP sizing;
- Electron beam 798 and electron beam 74A resins prepregged onto Hexcel's R-sized, AS4-R 12K fiber.

These selections were made in an effort to cover the full spectrum of promising solutions with a manageably small experimental matrix.

A three-tiered test battery was planned, with each tier eliminating certain material combinations and subsequent testing tiers becoming more demanding. First tier testing included basic, easily measured properties such as SBS strength, 0° flex properties, and void content/resin content/ fiber volume at room temperature. Second tier testing interrogated various hot-wet properties. Third tier testing added end notch flexure and transverse tensile tests at room temperature, plus additional hot-wet tests not conducted in second tier testing.

Adhesion results are shown in Table 3. For each potential solution, approximately 10 lbs of fiber was treated and shipped to YLA for prepregging. The 3K resin system was chosen because it was felt to be the best, rounded resin system available at the time. The improved resin systems, such as 800E were not sufficiently tested to warrant use at the time of the decision.

Once prepreg was made by YLA, it was shipped to Boeing for panel fabrication and electron beam curing. Panels were created and sent to AFRL for cut-up and testing. The initial set of panels had fairly low quality, so a second set were made, with marginal improvements. Due to time and budget constraints, the best panels were then tested. Unfortunately, during these trials, the isocyanate panel did not cure during radiation, so a 6" x 6" panel from the original trials was tested. The results of these tests are provided in Table 3.

Table 3. Adhesion Scale-Up Results

Panel #	Resin	Fiber Treatment	Round 1 Testing				Round 2 Testing			
			Transverse Strength (ksi)	SBS Strength (ksi)	Fiber pullout (see Figure 5)	Void Content estimate (%)	Transverse Strength (ksi)	SBS Strength (ksi)	Fiber pullout (see Figure 5)	Void Content estimate (%)
1	3K	Sol Gel (DOM = July 16th, 2002)	3.85		Moderate	>5	4.15	8.41	Medium to low	3.2
2	3K	Plasma	4.87	9.32	Moderate	approx 2	5.27	9.13	Near zero	3.7
3	3K	Sol Gel (DOM = July 19th, 2002)	5.58	8.82	Moderate	<1	5.66	10.31	Near zero	1.5
4	3K	GP	4.39	10.1	Extreme	<1	4.82	11.45	Extreme	1.3
6	3K	ATI - 9307	4.74		Extreme	approx 2	4.57	9.76	Extreme	2.0
7	3K	ORNL1	3.72		Extreme	approx 2	4.43	9.69	Extreme	1.5
7'	3K	ORNL1 - 160°F debulk	2.28		Extreme	>5				
8	3K	ORNL2	4.49	9.77	Extreme	<1	4.33	10.30	Extreme	1.2
8'	3K	ORNL2 - 160°F debulk	3.83		Extreme	>5				
IM7/9773	977-3	GP	9.3 - 9.6	18-19	Low to zero	<0.05				
AS4/3501-6	3501-6	GP	8.9	18-19	Low to zero	<0.05				
IM7/5250-4	5250-4	GP	10	20	Low to zero	<0.05				

Because tier 1 tests did not satisfy the project goals, tier 2 and 3 tests were not conducted. While these results were not as successful as we had hoped, there is promise in Plasma #2 and Sol-Gel #3 in that they showed some increase in transverse tensile performance and an improvement in the fiber pull-out typical of e-beam cured composites. Some of the disappointing results were attributed to lack of familiarity with processing the new materials. In many cases, application of newly developed fiber treatments and prepregging with them was challenging, as the new treatments changed the fiber/prepreg processing characteristics. Even with materials for which there is historical experience, often "dialing in" the process requires substantial time and material, and when one is working with limited quantities of unfamiliar material, this becomes a serious problem.

It is clear that these results in combination with the solutions developed in the Adhesion IPT will serve as a solid foundation for continued incremental property improvements of electron beam cured composites in the future.

4.7. Irradiation

The irradiation team provided data and irradiation support for the other IPT's. Several irradiators were available, which allowed irradiation under a variety of conditions to explore sensitivity to irradiation parameters. Most irradiation was performed on electron accelerators, however gamma cell irradiators are also useful as screening tools. Various electron accelerator and gamma cell parameters available to the project team are tabulated in Appendix C.

A simple software program was written to simulate the irradiation of a product conveyed through the beam. The program simulates beam pulsing, scanning, and dose profile within the beam spot to calculate the maximum dose applied to the part. With further code development, it would be quite simple to use this code to ascertain whether the irradiation parameters uniformly distribute dose to the part's surface. As presently written, the code determines the dose applied at a particular point, and manual repetition is required to determine dose at multiple points. Data was obtained for four of the electron accelerators and the code was validated against the results. The simulation results agreed closely with the results from all accelerators except the STERIS Rhodotron. The discrepancy on the Rhodotron is believed to be related to its use of secondary bending magnets. As shown in Figure 6, the beam (represented by dotted red lines) is bent by secondary magnets (not shown) at the beam exit, so that the beam is normal to the conveyor when it enters the irradiation target. The other accelerators lack this feature.

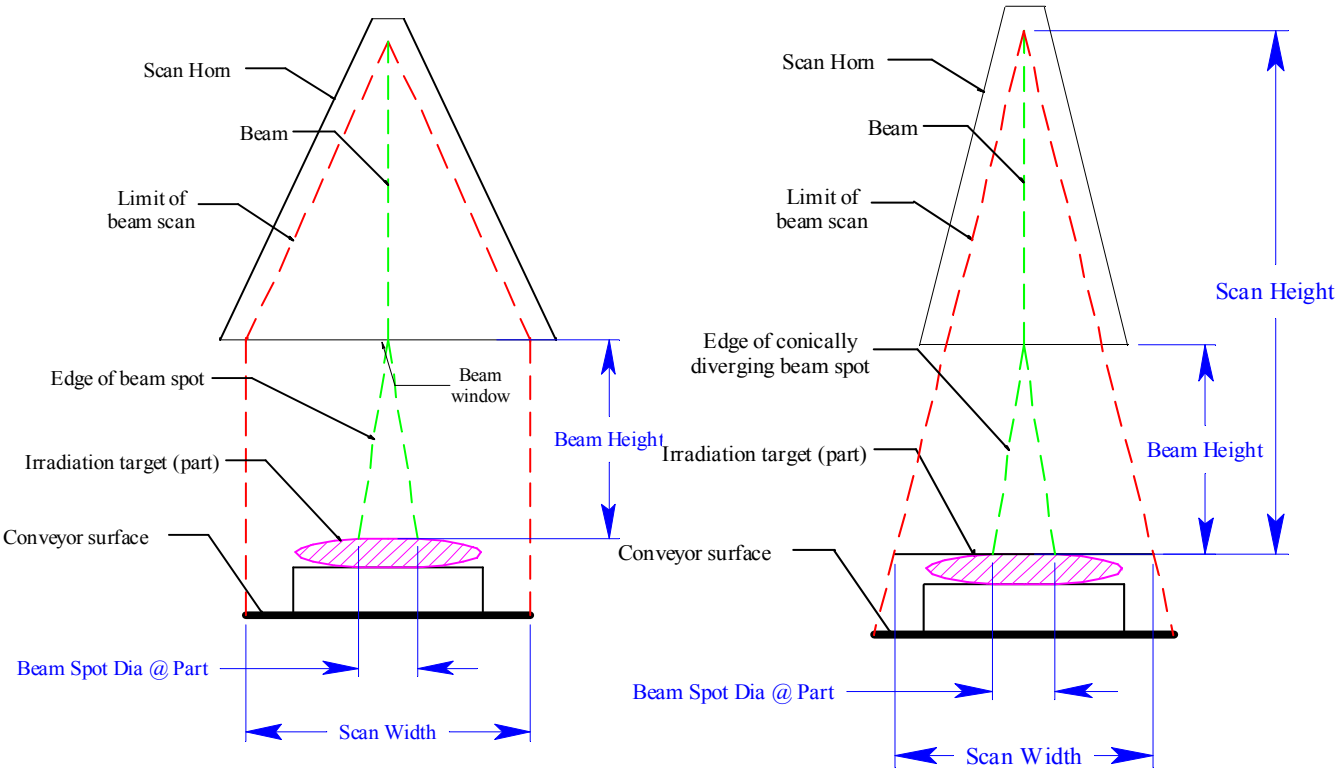

Figure 6. Beam path in Rhodotron (left) vs. other project accelerators (right).

The radiation simulator requires input that includes beam spot dimensional information and dose rate profile within the beam spot. Usually, the beam spot can be assumed to be circular or elliptical, with spot dimensions increasing proportionally with distance from the vacuum window. In this case, a single measurement of the beam spot dose profile, such as that shown in Figure 7, is sufficient to enable accurate calculation of most irradiation cases. As with most accelerators, the dose profile in Figure 7 can be mathematically approximated by a Gaussian function, The Rhodotron's secondary bending magnets affect the flight path of electrons near the beam exit, and may render invalid the normal mathematical assumptions, specifically Gaussian dose profile in the beam spot, and proportionality of spot dimensions with distance from vacuum window. The discrepancy was not deemed sufficiently important to justify the effort of making additional measurements on the Rhodotron. Further development of the radiation simulation code and validation for Rhodotron accelerators may be a worthy topic for future investigation, for example as a university class project.

As part of its effort to ensure a standardized irradiation process with detailed data records, the irradiation team developed a standard log sheet for composites curing. The standard log sheet is included in Appendix D. A glossary of standard terms was also developed, and is included as Appendix E. All terms in the log sheet should be interpreted according to the glossary.

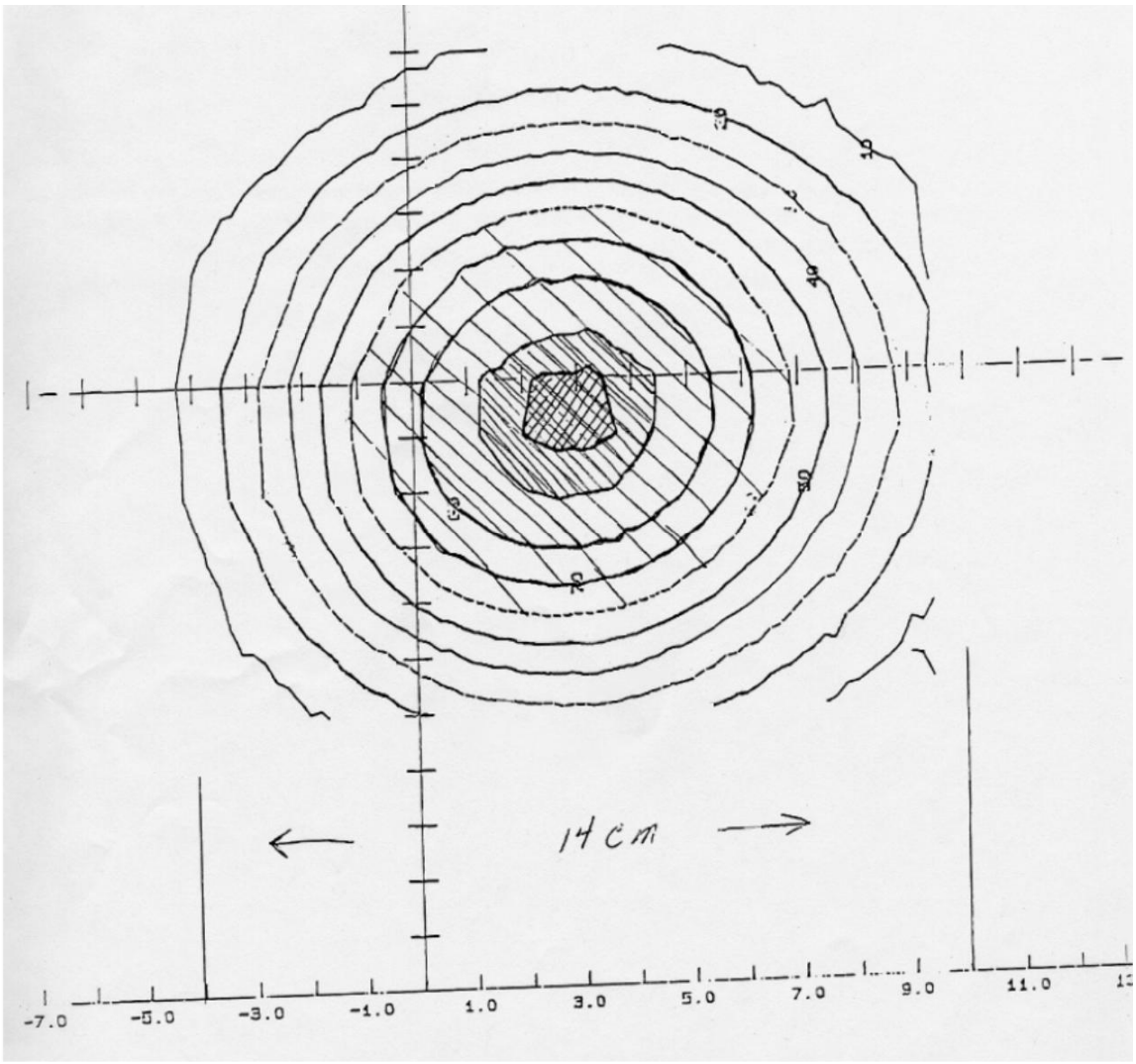

Figure 7. Conveyor level dose profile in beam spot for Acsion I10/1 accelerator.

4.8. Kinetics

4.8.1. Kinetics IPT Mission

The mission of the Kinetics IPT was to characterize and understand the reaction kinetics and mechanisms of electron beam cured epoxy resins by identifying initiation, propagation, and termination reactions during cationic polymerization. The lack of understanding of the cure mechanisms associated with cationic radical propagation in epoxide networks hinders the capability of technical designers to predict final performance of the cured products. Therefore, kinetics investigations can provide baseline information to a kinetics model that allows predictive capability for degree of cure, extent of cure, etc. in a cationic initiated composite matrix at various initiator concentrations.

4.8.2. Kinetics Technical Strategy

The kinetics investigation sought to establish the causal effects that lead to final products and network conversion in electron beam initiated cationic cure of epoxy-based systems. The

model systems investigated include a monofunctional epoxide, phenyl glycidyl ether (PGE), which forms linear and soluble products after irradiation, and a common difunctional epoxide, diglycidyl ether of bisphenol A (DGEBA). The DGEBA selected during this study was Tactix 123, in order to correlate relevant results with other components of the project evaluation.

In order to divide the kinetics investigations along technical barriers, the overall developments and experiments were pursued at one of three molecular levels.

1. Molecular kinetics – This investigation sought to establish the molecular pathways and intermediate molecular species that were involved in the cure progression. The most basic level of investigation in this study included decomposition products of the initiator. Additionally, chemical intermediates of initiator reaction with epoxide were sought.
2. Macro-kinetics (performed in conjunction with irradiation) – This investigation sought to develop the initial database for electron beam process parameters and the influence of variations in such control variables as dose, dose-rate, and temperature rise on polymerization of systems. Additionally, one can assume that concentration of initiator also falls into this tier of investigation, as well as any resin contaminants that may be present in the bulk resins.
3. Kinetics modeling approach – This investigation sought to incorporate any determined information from levels I and II into a predictive model that allows engineers and designers to select cure processing conditions, monomer to initiator ratios and other basic design criteria for generating commercial level products using electron beam irradiation.

4.8.3. Molecular Kinetics Investigations

Steady state γ-radiolysis and time-resolved pulse radiolysis/optical detection techniques were used to obtain information on the nature of intermediates formed by the photoinitiator and PGE. Steady state γ-radiolysis and pulse radiolysis measurements were performed at the DOE-funded Notre Dame Radiation Laboratory in South Bend, Indiana.

4.8.3.1. Molecular Kinetics Results

γ-Radiolysis of CD-1012- Previous researchers have proposed that cationic polymerization of epoxy resins can proceed via protonation of the oxygen atom of the epoxy ring by $HSbF_6$, a strong acid produced upon radiolysis of CD-1012.[14,15] In order to test for the formation of acid upon degradation of CD-1012, we examined γ-radiolysis of CD-1012 in methanol using bromophenol blue as an acid indicator. Bromophenol blue has a strong absorption at 596 nm in neutral media. As the acidity of the media is increased, the absorption at 596 nm decreases indicating a change in the pK_a of the solution. If CD-1012 absorbs the γ-radiation and undergoes degradation to species that can generate $HSbF_6$, then one should observe a decrease in the absorption at 596 nm. When a solution of CD-1012 in methanol ($5x10^{-4}$ M) containing bromophenol blue ($9x10^{-5}$ M) was subjected to γ-radiation (using 1, 5, and 20 kRad/min dose rates), a decrease in the absorption of bromophenol blue at 596 nm was observed. This decrease in absorption was a function of radiation time, suggesting that the formation of acidic species whose concentration increased as irradiation time increased. Figure 8 shows a representative plot of the change in absorption spectra of bromophenol blue as a function of total dose for CD-1012 in methanol. Such observation is in good agreement with the formation of $HSbF_6$ upon γ-radiolysis of CD-1012.

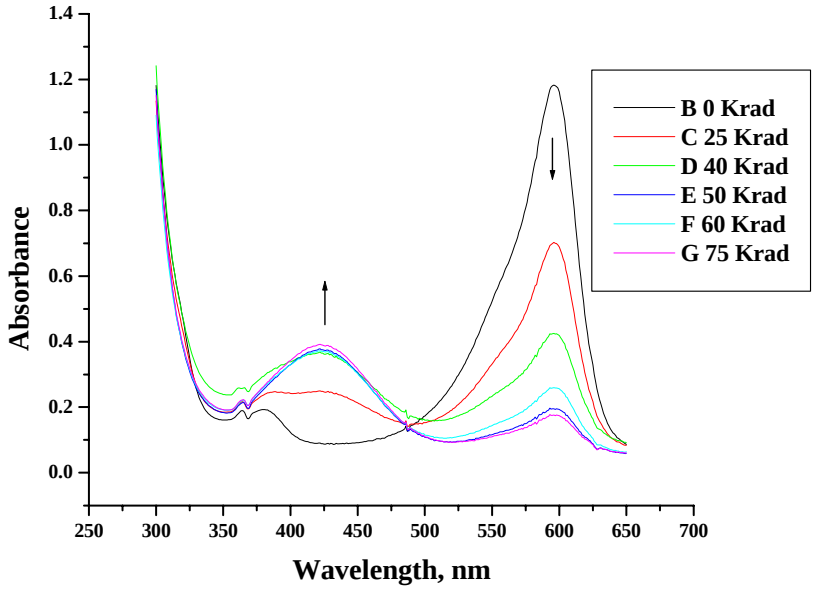

Figure 8. Changes in the absorption spectra of bromophenol blue in methanol upon γ-radiolysis of CD-1012 using 1 kRad/min source, [CD] = 5E-4 M, [BPB] = 9 E-5 M.

Pulse radiolysis of PGE. Decay of the transient absorption spectrum obtained upon pulse radiolysis of degassed PGE is shown in Figure 9. The transient spectrum observed 0.5 μs after the electron pulse exhibits peaks at 300, 333 (sh), and 400 nm. The 333 nm absorption is buried under the intense 300 nm band and appears at 0.5 μs after the pulse as a shoulder. A broader band with intensity much smaller than that of 300 nm is observed in the 400 to 500 nm wavelength region. The transient spectrum changes significantly 3.0 μs after the pulse. Most of the spectral features, however, resemble the spectrum observed at 0.5 μs after the pulse, except for a broad band. At longer times (> 50 μs), the transient spectrum does not change significantly. Based on the observed transient spectra, it is clear that the major absorption band (300 nm) corresponds to the first intermediate formed and the broad bands at 400 nm and higher to a second intermediate. Assuming that the spectral features of the first intermediate are the same throughout the observed time scale and that the 300 nm absorption band is mostly due to this species, we can deduce the spectral features of the second intermediate by subtracting the normalized spectrum obtained at 160 μs after the pulse from the normalized spectrum obtained at 0.5 μs after the pulse (both spectra normalized at 300 nm). The subtracted spectrum (Figure 10) representing the second intermediate exhibits absorption bands at 310, 340 and 430 nm, respectively.

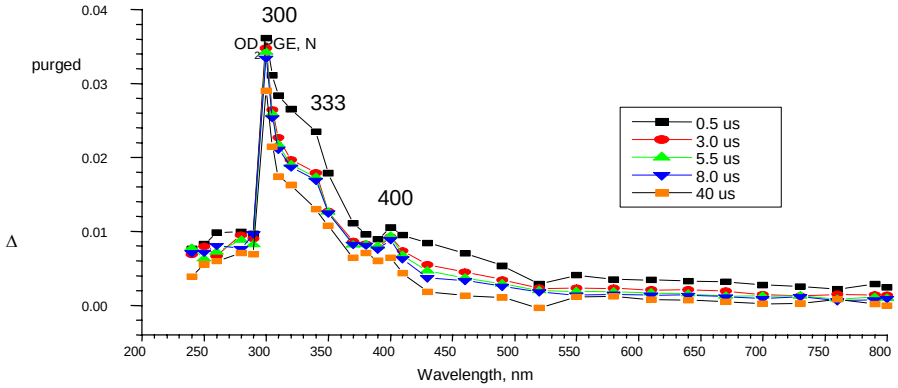

Figure 9. Transient absorption spectrum of nitrogen-saturated PGE obtained at various times after the pulse.

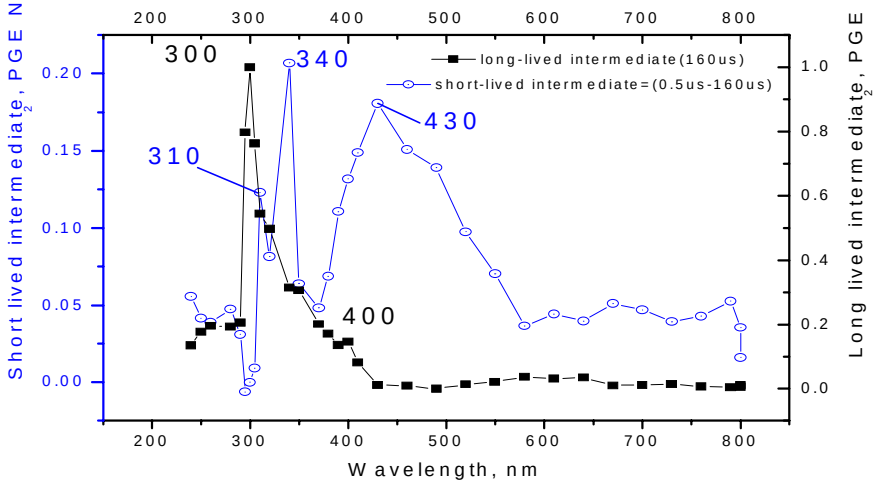

Figure 10. Transient absorption spectra of short-lived and long-lived intermediates obtained upon pulse radiolysis of PGE.

Pulse Radiolysis of Degassed PGE Containing 3% (wt) CD-1012. The evolution and decay of the transient absorption spectrum of degassed PGE in the presence of 3 weight-percent CD-1012 shows spectral features with maxima at 360 and 400 nm which change with time (not shown). Growth of the 400 nm absorbance maximizes in approximately 11 μs after the pulse and decays on a much longer time scale. At longer times (>20 μs after the pulse), the 435 nm band becomes a major absorption band in the transient spectrum and decays on a much longer time scale. About one third of the transient spectrum decayed within 160 μs (limits of pulsed probe lamp). Similar spectral changes were also observed for the transient in the 500 to 800 nm wavelength region (not shown). This transient exhibits a maximum absorption at λ_{max} > 800 nm and two shoulders at 605 and 685 nm (not shown). Spectral features of these intermediates change with time. At 160 μs after the pulse, only the spectrum of transient with λ_{max} > 800 nm is still observed. We observe significant variation in the rise-time of transients (e.g., from 2 μs for

605 nm absorbance to 20 μs for 435 nm band). Almost all the absorption bands reach their maximum value between 20 and 60 μs after the pulse, suggesting that these transients are formed by secondary processes.

Tentative Assignment of Intermediates Observed on Pulse Radiolysis of Degassed PGE Containing 3% CD-1012. None of the transients previously assigned to PGE (9, 9a, 10, and 10a in Figure 11 –Scheme I) were observed in the pulse radiolysis of PGE containing 3% CD-1012. Such observation suggests that at this concentration of CD-1012 all PGE intermediates are intercepted by CD-1012, leading to the observed transients shown in Figure 12 – Scheme II. Additional intermediates are produced by the reduction of iodonium salt with solvated electrons (Scheme II). Products of this reaction are an aryl radical 13, hexafluoroantimonate anion 14, and an aryl iodide 12. A strong Brönsted acid, 15 ($HSbF_6$), is also generated upon hydrogen abstraction from the PGE molecule by hexafluoroantimonate anion (14). The polymerization reaction shown in Scheme II proceeds through the reduction of iodonium salt, Ar_2ISbF_6, by either radicals 9, 9a, 10, 10a or by the solvated electrons producing the intermediates 11 and 11a. The products of this reaction are an aryl radical 13 and hexafluoroantimonate anion 14 and an aryl iodide 12. The aryl radical 13 could abstract a hydrogen atom from a molecule of PGE 1 to produce intermediates 4 and 4a, which can proceed to form polymer according to Scheme II. Alternatively, acid-catalyzed ring opening of the epoxy proceeds through intermediate 16, which has 14 as a counter ion. Ring opening can take place to generate two different intermediates 17 and 17a. Interaction of a PGE molecule with either 17 or 17a can produce intermediates 18 or 19, starting a repeating unit of polyphenylglycidyl ether (PPGE). The observed absorption in the 300 to 600-nm region can be assigned to either intermediates 11 and 11a, or intermediates 17 and 17a with 14 as a counter ion. However, the fact that there is no significant absorbance in the 300-nm region, where ketyl intermediate absorbs, suggests that intermediate 17 is the most likely candidate. It also indicates that initiation of cationic polymerization by PGE radicals is not very efficient compared to polymerization initiated by the reaction of CD-1012 with solvated electrons. The broad absorption band around 605 nm could be attributed to the absorption of diaryliodonium radical cation based on the literature data. It is also plausible that the radiolysis of PGE in the presence of 3% CD-1012 does not proceed to give the first intermediate (9, 9a, 10 and 10a in Scheme I). The precursor of this intermediate, which is the oxygen sensitive component of the second intermediate, reduces CD-1012, producing the same combination of intermediates 12, 13, and 14 as well as ring opening of the epoxy ring without the formation of a ketyl intermediate. This is consistent with our experimental observation that the observed transient obtained at 0.75 μs after the pulse (for PGE + CD-1012 mixture) shows no spectral features of the first intermediate. Table 4 summarizes the spectral features and lifetimes of these intermediates and their components.

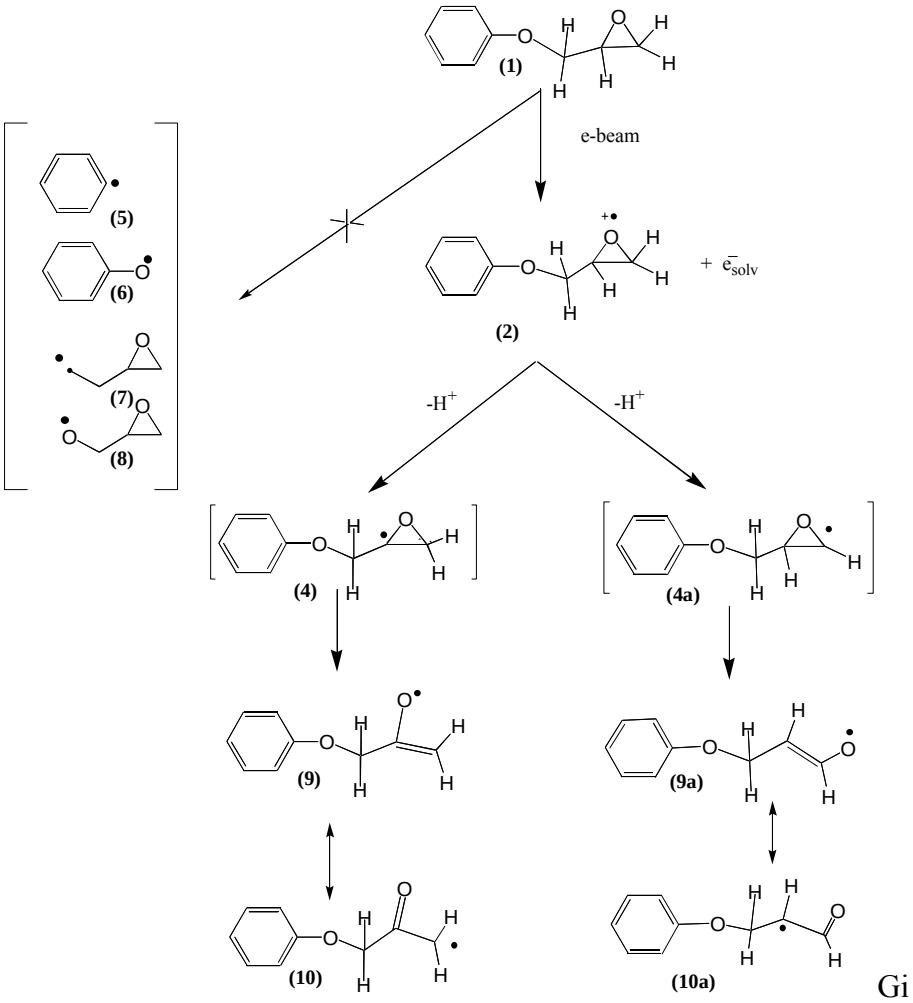

Figure 11. Scheme I - plausible intermediates produced by pulse radiolysis of PGE.

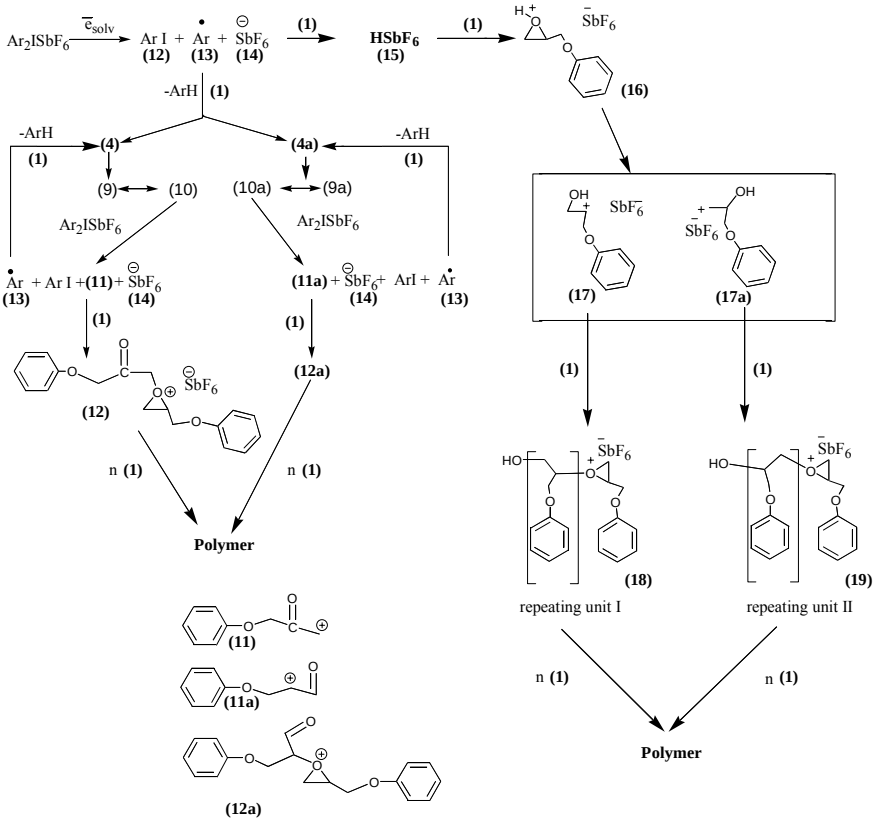

Figure 12. Scheme II – plausible intermediates produced by pulse radiolysis of 3% CD-1012 in degassed PGE.

Table 4. Spectral features and the lifetime of intermediates observed for PGE and PGE/CD-1012 by pulse radiolysis

Transient Observed	CD-1012 Present	Components Present	Absorption Peaks Observed nm	Quenched by Oxygen	Lifetimes (μs)
1	No	1	300(sharp), 400 (shoulder), 450-700 (broad)	No	3.6-8.6 μs 70-90 μs
2	No	2	340 (sharp) 430 (sharp)	Yes No	1, 70 μs 1- 5 μs, 60-7070μs
1	Yes	ND*	360 (sharp) 400 (sharp) 500-800 (broad)	ND*	ND*

ND* not determined.

4.8.3.2. Molecular Kinetics Conclusions and Future Works

The kinetics results have shown that steady state and time resolved pulse radiolysis techniques were utilized to obtain useful information on the nature of intermediates involved in the polymerization process. γ-radiolysis of CD-1012 results in its decomposition and produces a strong acid ($HSbF_6$), which can protonate the epoxy oxygen and initiate cationic polymerization process. Time resolved pulse radiolysis with optical detection has revealed that upon absorption of the e-beam radiation PGE (in the absence of CD-1012 photoinitiator) produces at least two transients, which show characteristics of cation radical as well as radical species. A similar study in the presence of CD-1012 has shown that at least one of the intermediates initially formed by PGE may be rapidly trapped by CD-1012 to produce other intermediates that can initiate polymerization process. The lifetime of intermediates identified by pulse radiolysis with optical detection techniques are in the range 1 to 90 μs.

The results reported herein represent a good start to molecular kinetics studies, but much additional work is needed. Future work should focus on the effect of dose rate (γ-radiolysis) and total dose on decomposition rate of CD-1012. Pulse radiolysis with optical detection techniques should also be utilized to identify the intermediates (besides $HSbF_6$ formation) formed by CD-1012 upon e-beam absorption. Pulse radiolysis with EPR should be used as a complementary technique to pulse radiolysis with optical detection to identify and characterize the intermediates with radical character formed during e-beam radiation of PGE and PGE/CD-1012.

4.8.4. Kinetics-based process modeling

Many of the most attractive features of electron beam curing arise from the potential of unparalleled flexibility this process offers with respect to processing temperatures and rates of reaction. This flexibility means that, as required, electron beam irradiation can potentially cure components quickly or slowly, at high or low temperature, and even selectively cure sections of a component if required. However, the same features of electron beam curing that lead to this flexibility also lead to the complexity that is potentially one of its biggest drawbacks. The numerous interacting phenomena involved in radiation curing of polymers and composites make it very difficult to predict *a priori* the appropriate process conditions required to produce high-quality robust components.

A promising approach to addressing this issue is the application of physics-based processing models. Such process models have been used to simulate numerous composites manufacturing processes and can predict such parameters as temperature and resin cure rate during processing, resin flow, and the prediction of residual stress and deformation. These models have been demonstrated to be valuable tools for both composites researchers and manufacturers in facilitating a deeper understanding of processing phenomena and in development of highly optimized, robust processes.

In this work, a very simple one-dimensional process model was developed to predict temperatures and cure rates during electron beam processing of polymers and composites. The primary intent for this model is to act as a simple tool for electron beam curing researchers for study of potential radiation cure process variants and to improve understanding of the interaction of various phenomena involved in electron beam curing.

The governing equation of the developed process model is the standard one-dimensional transient heat conduction equation, with a volumetric heat generation term, as follows:

$$\frac{\partial}{\partial t}(\rho C_p T) = \frac{\partial}{\partial z}\left(k_z \frac{\partial T}{\partial z} \right) + \dot{Q}$$

where ρ is the material mass density, C_P is the specific heat capacity and k_z is the material *z*-direction (through thickness) thermal conductivity. $\dot{Q}$ is the volumetric heat generation, which is a combined effect of the thermal energy imparted to the composite by impinging electrons and the resin exothermic reaction, $\dot{Q}_C$, calculated from:

$$\dot{Q}_C = \frac{d\alpha}{dt}(1 - V_f)\rho_r \Delta H_R$$

where V_f is the fiber volume fraction, ρ_r is the resin mass density, α is the resin degree of cure, and ΔH_R is the resin *heat of reaction*, defined as the total amount of heat evolved during a "complete" resin reaction.

The cure rate equation used in the current model is equivalent to that developed by Palmese and co-workers[16, 17] at Drexel University, and is of the form:

$$\frac{d\alpha}{dt} = k_p \cdot (1 - \alpha) \cdot I$$

where k_p is a reaction rate constant with an Arrhenius temperature dependency and I is the concentration of activated photoinitiator. The rate of formation of activated photoinitiator is calculated using:

$$\frac{dI}{dt} = k_i \cdot (C_0 - I)$$

where C_0 is the starting initiator concentration. The initiation rate constant, k_i, is assumed to be directly proportional to the (time-averaged) dose rate and independent of both initiator concentration and cure temperature.

At the onset of this project, no practical method existed for *in-situ* monitoring of the electron beam curing process (an *in-situ* NIR technique has since been developed by Palmese and co-workers[16,17]). Hence, in order to derive the cure model constants and to verify model predictions, it was necessary to undertake the development of a simple "electron beam calorimeter". Two generations of an experimental device were produced, the second of which is shown in Figure 13. This calorimeter consists of a series of very lightweight cylindrical polyurethane foam blocks into which resin-filled polypropylene syringes are embedded. During irradiation, thermocouples within the syringes measure the temperatures of uncured or pre-cured resin. Using these temperature measurements, a finite-difference based numerical analysis was developed which calculates both electron beam dose rate and resin cure rate.

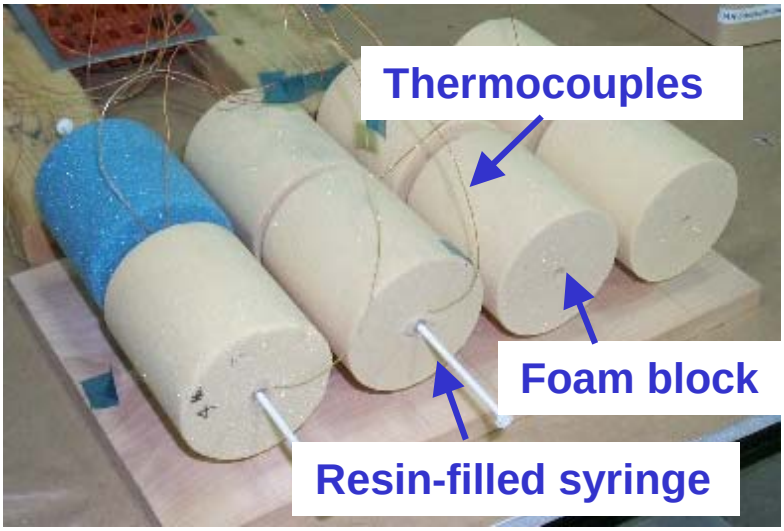

Figure 13. Electron Beam Cure Calorimeter.

Using this calorimeter, a series of electron beam irradiation process trials was undertaken on various DGEBA-based resins. Varied process conditions included dose rate, total dose, resin moisture content and initial resin temperature. Comparisons between experimental measurements and model predictions showed good "qualitative" agreement, with processing parameters having the predicted effect on cure rates. However, as shown in Figure 14, some important differences in predicted and measured absolute temperatures and cure rates are apparent, particularly for neat resins.

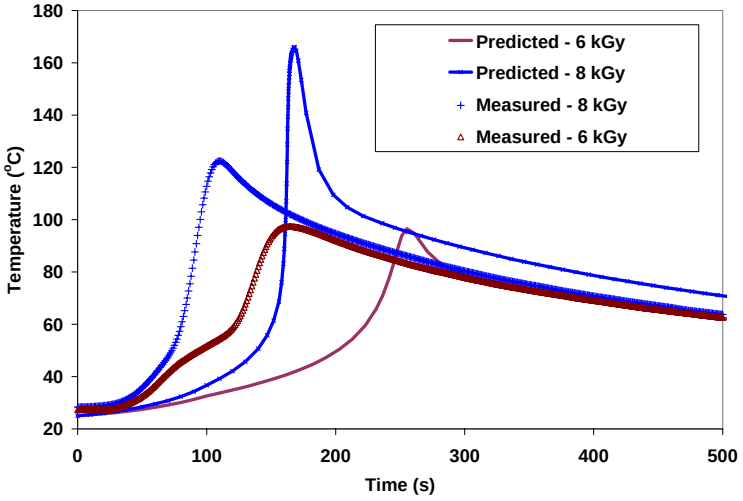

Figure 14. Comparison of Predicted and Measured Syringe Temperatures (6 kGy and 8 kGy total dose), Tactix 123 resin with 3 phr CD1012 initiator.

Efforts at reconciling experimental measurements with model predictions are continuing. However, even at this early stage, the model has shown its potential as a useful research and development tool. By serving as a simple method for exploring the very complex and sometimes subtle interactions between temperature, dose rate, and cure rate, the process model is expected to provide insight into the process that is otherwise difficult to acquire.

The current version of the process model is available to users as a simple windows-based executable code with text-file-based inputs and outputs. A simple visual interface is under development, but it may be some time before it is available. As more confidence in the model fundamentals are developed, and as the potential users of the model are better defined, it is hoped that a more comprehensive and geometrically complex version will be developed.

Final refinements to a "second generation" electron beam calorimeter and its accompanying software were completed in 2003. Although still somewhat crude in comparison to conventional instruments, this calorimeter provides reasonably accurate cure rate measurements during electron beam processing and is very inexpensive and easy to use.

5. SUBJECT INVENTIONS AND PUBLICATIONS

5.1. Subject Inventions

1. Chris J. Janke, "Novel Adhesion Enhancing Fiber Sizings, Primers, and Coatings"
2. Chris J. Janke, "Rapid SRIM Processing Method Using Radiation or Thermal Pre-Activated Cationic Initiators and Epoxy Resins"
3. B. Defoort and L. T. Drzal, "Plasma Treatment of Carbon Fibers for Use in Electron-Beam Cured Composites"
4. B. Defoort and L. T. Drzal, "Aldehyde Based Sizings for Carbon Fibers"
5. B. Defoort and L. T. Drzal, "Carbon Fiber Surface Treatment to Promote Adhesion for Electron Beam Processed Epoxy Composites"
6. B. Defoort and L. T. Drzal, "Surface Treatment of Carbon Fibers Using Ultraviolet Light in Ozone for Electron Beam Processed Polymer Composites"

5.2. Publications

1. J. H. Chen, A. Johnston, L. Petrescue and L. Bordovsky, "Development of a Calorimeter for in-situ Cure Monitoring of Electron Beam Curing of Polymers", Proceedings of the 4th Canadian-International Composites Conference, CANCOM 2003, Ottawa, ON, August 19-22, 2003
2. B. Defoort. And L. T. Drzal, "Influence Of Processing Conditions On Adhesion Between Carbon Fibers And Electron-Beam Cured Cationic Matrices," J. Adhesion 79(4) 361-382 (2003)
3. K. C. Cole, M.-T. Ton-That, A. Johnston, M. Hojjati, K. Valcourt, V. Lopata, "Investigations into the Mechanism of Electron-Beam Curing of an Epoxy Resin", Proc. Fourth Canada-Japan Workshop on Composites, Vancouver, British Columbia, Canada, Sept. 19-21, 2002, Pages 43-52
4. C.J. Janke, "Status Report - Electron Beam Interface CRADA", AFOSR E-Beam Panel Discussion, 47th International SAMPE Symposium 2002, May 12-16, 2002, Long Beach, CA, 47, (2002)

5. B. J. Frame, G.E. Wrenn, and C.J. Janke, "Results of Electron Beam Prepreg Debulking Study", 47th International SAMPE Symposium 2002, May 12-16, 2002, Long Beach, CA, 47, (2002)
6. R. Foedinger, T. Schneider, R. Grande, S. Malghan, T. Walton, R. Norris, B. Frame, C. Janke, and R. Evans, "Development of Electron Beam Curable Composite Motor Cases", 47th International SAMPE Symposium 2002, May 12-16, 2002, Long Beach, CA, 47, (2002)
7. R. Dabestani, I.N. Ivanov, and J.M. Sands, "Application of Time-Resolved Pulse Radiolysis Technique in the Investigation of the Mechanism of Epoxy Resins Cationic Polymerization", 47th International SAMPE Symposium 2002, May 12-16, 2002, Long Beach, CA, 47, (2002)
8. A. Johnston, K.C. Cole, M. Hojjati, M. Mascioni, G. R. Palmese, and V. J. Lopata, "A Basic Process Model for Electron Beam Curing of Composite Materials", 47th International SAMPE Symposium 2002, Long Beach, CA, May 12 – 16, 2002
9. B. Defoort, R. S. Schalek, and L. T. Drzal, "A TEM Investigation of the Network Structure of Electron Beam Cured Epoxy Polymers", Microscopy Society of America 2002 *(Abstract Only)*
10. B. Defoort and L. T. Drzal, "Problems And Solutions To Carbon Fiber-Matrix Adhesion In Electron-Beam Processed Composites," Proceedings of the Annual Technical Meeting Adhesion Society, v.25, Orlando, Florida, February 2002 The Adhesion Society, pp 334-336
11. L. T. Drzal, B. Defoort, M. J. Rich, and K. Thayer, "Fiber-Resin Adhesion in Radiation Cured Composites", Final report no. MSU-OIP 02002-02005F, College of Engineering, Composite Materials and Structures Center, Contract # 4500009854
12. B. DeFoort and L. T. Drzal, "Interfacial Phenomena and Fiber-Matrix Adhesion in Electron Beam Processed Composites", Proc. 33nd International SAMPE Technical Conference. Advancing Affordable Materials Technology, Vol. 33, Seattle, WA, November, 5.8, 2001. Society for the Advancement of Material and Process Engineering, pp. 292-303
13. C.J. Janke, R.D. Lomax, S. Robitaille, S. Duggan, R.C. Serranzana, V.J. Lopata, "Improved Epoxy Resins Cured by Electron Beam Irradiation", 46th International SAMPE Symposium 2001, May 6-10, 2001, Long Beach, CA, 46, 2048 (2001)
14. R. Dabestani, I.N. Ivanov, "Cure Kinetics of Cationic Polymerization of Phenyl Glycidyl Ether (PGE) and Tactix 123 Using CD-1012 as Photoinitiator", 46th International SAMPE Symposium 2001, May 6-10, 2001, Long Beach, CA, 46, 2075 (2001)
15. V. Bechel, C.J. Janke, M. Wilenski, G.P. Tandon, "Constituent Level Examination of an E-Beam Cured Graphite/Epoxy Composite", 46th International SAMPE Symposium 2001, May 6-10, 2001, Long Beach, CA, 46, 2115, (2001)
16. B. DeFoort and L. T. Drzal, "Adhesion Between Carbon Fibers and Cationic Matrices in Electron Beam Processed Composites", 46th International SAMPE Symposium 2001, May 6-10, 2001, Long Beach, CA, 46, 2063, (2001)
17. B. DeFoort and L. T. Drzal, "Influence of Thermal Post Curing on Electron Beam Cured Composites", 46th International SAMPE Symposium 2001, May 6-10, 2001, Long Beach, CA, 46, 2550, (2001)

18. A.J. Berejka, C. Eberle, "Electron Beam Curing of Composites in North America", 12th International Meeting on Radiation Processing, March 2001, Avignon France, published in J. Radiation Physics and Chemistry, 63, 551 (2002)
19. B. Defoort and L. T. Drzal, "Influence of Processing Conditions on the Electron Beam Curing Kinetics of an Epoxy Resin for Composites", Pacifichem 2000 - Radiation Chemistry Of Polymers, Hawaii, December (2000) *(Abstract Only)*
20. B. Defoort and L. T. Drzal, "Adhesion between Carbon Fibers and Cationic Matrices in Electron-Beam Processed Composites", SAMPE Automotive Conference 2000, Paper D-20
21. C.J. Janke, "Results on Improving the Toughness of E-Beam Curable Cationic Epoxy Resins", 2000 Electron Beam Curing Workshop, June 14-15, 2000, Oak Ridge, TN
22. V. Lopata, C. Eberle, S. Korenev, M. Stern, M. Wilenski, "Critical Irradiation Parameters", 2000 Electron Beam Curing Workshop, June 14-15, 2000, Oak Ridge, TN
23. C. Eberle, "Interfacial Properties of Electron Beam Cured Composites", 2000 Electron Beam Curing Workshop, June 14-15, 2000, Oak Ridge, TN
24. R.E. Norris, "E-Beam Cure Monitoring – A Brief Overview of the Issues and Possibilities", Proc. 4th Electron Beam Curing of Composites Workshop, 14 – 15 June 2000, Oak Ridge TN
25. L. T. Drzal and B. Defoort,, "Interfacial Phenomena and Adhesion of Carbon Fibers to Epoxy Matrices in Electron Beam Processed Composites," Proc. 4th Electron Beam Curing of Composites Workshop, 14 – 15 June 2000, Oak Ridge TN
26. M.S. Wilenski, C. Eberle, S. Korenev, V. Lopata, M. Stern, "A Method for Specifying Consistent Radiation for the Processing of Electron Beam Cured Composites", 45th International SAMPE 2000 Symposium, May 21-25, 2000, Long Beach, CA, 45, 1888, (2000)
27. R. Dabestani, "Synthesis of High Performance Polymer Composites by Electron Beam Curing", Proc. E-Beam Curing Kinetics Workshop, 13 April 2000, Newark DE
28. L. T. Drzal, M. J. Rich, and E. K. Drown, "Possible Mechanisms Responsible For Low Levels of Adhesion Between Carbon Fibers And Epoxy Matrices In E-Beam Processed Composites," 44th International SAMPE Symposium 1999, May 23-27, 1999, Long Beach, CA, 44, 157 (1999)

6. COMMERCIALIZATION POSSIBILITIES

Commercialization of electron beam curing technology is already in its early stages, with some applications in field testing at this time. High performance aerospace applications are likely to lead the early commercialization, followed by migration to lower cost, consumer-driven applications. The improvements made in this project and subsequent work are expected to be quickly implemented as part of the total technology commercialization.

7. PLANS FOR FUTURE COLLABORATION

A number of the project participants are continuing to collaborate in the development of electron beam curing technology. Formal collaboration is dependent on availability of funding.

8. CONCLUSIONS

The project team made several important discoveries. A number of fiber coatings or treatments were developed that improved fiber-matrix adhesion by 40% or more, according to microdebond testing. The effects of dose-time and temperature-time profiles during the cure were investigated, and it was determined that fiber-matrix adhesion is relatively insensitive to the irradiation procedure, but can be elevated appreciably by thermal postcuring. Electron beam curable resin properties were improved substantially, with 80% increase in electron beam 798 resin toughness, and ~ 25% and 50% improvement, respectively, in ultimate tensile strength and ultimate tensile strain vs. earlier generation electron beam curable resins. Additionally, a new resin electron beam 800E was developed with generally good properties, and a very notable 120% improvement in transverse composite tensile strength vs. earlier generation electron beam cured carbon fiber reinforced epoxies. Chemical kinetics studies showed that reaction pathways can be affected by the irradiation parameters, although no consequential effects on material properties have been noted to date. Preliminary thermal kinetics models were developed to predict degree of cure vs. irradiation and thermal parameters. These models are continually being refined and validated.

Despite the aforementioned impressive accomplishments, the project team did not fully realize the project objectives. The best methods for improving adhesion were combined with the improved electron beam 3K resin to make prepreg and uni-directional test laminates from which composite properties could be determined. Nevertheless, only minor improvements in the composite shear strength, and moderate improvements in the transverse tensile strength, were achieved. The project team was not satisfied with the laminate quality achieved, and low quality (specifically, high void fraction) laminates will compromise the composite properties. There were several problems with the prepregging and fabrication, many of them related to the use of new fiber treatments.

There remains a compelling need to resolve the deficient mechanical properties of electron beam curable polymer composites. The principal opportunities appear to be a continuation of the work reported herein, as follows:

Fiber treatment and prepregging – fiber treatment and production prepregging require significant quantities of material to get the process “dialed in”. Unfortunately, the bench-scale quantities of fiber treatment that were available to us did not, in many cases, allow us to make enough consistently treated fiber to make consistently high quality prepreg. We need to find a way around this problem.

Laminate fabrication – we found it very difficult to make void-free laminates. This was particularly surprising, given that formerly we had consistently made good laminates using the same fiber and resin. Good prepreg may solve the problem, but if not further work is needed on laminate fabrication.

Other resins – both the electron beam 798 and electron beam 800E resins are superb candidate resins. Perhaps one of these or another resin will yield notable improvements.

Reduced requirements – the exit criteria are exceedingly challenging. The immature electron beam curable materials technology is asked to reproduce performance that was achieved only after decades of thermally curable materials development. The electron beam curing community, including end users, are seriously discussing the possibility of lowering the resin’s service temperature requirement to make the remaining property targets more readily achievable.

The project team was sufficiently encouraged by the bench-scale adhesion and resin improvements that some of the partners are continuing to address these and other remaining barriers in an attempt to achieve satisfactory materials integration and scale-up and to realize the overall project objectives.

9. REFERENCES

1. C. J. Janke, R.E. Norris, K. Yarborough, S. J. Havens, V. J. Lopata; "Critical Parameters for Electron Beam Curing of Cationic Epoxies and Property Comparison of Electron Beam Cured Cationic Epoxies Versus Thermal Cured Resins and Composites", 42nd International SAMPE Symposium, Anaheim, CA, 42, 477 (1997)
2. C. J. Janke; "Properties of Electron Beam Cured vs. Autoclave Cured Composites and Adhesives," Proc. 2nd Electron Beam Curing of Composites Workshop, Oak Ridge, TN, Sept. 10-11, 1997
3. C. J. Janke, J. D. Farmer, V. J. Lopata; "The Electron Beam Cure of Fiberglass/Epoxy Prepregs", 29th International SAMPE Technical Conference, Orlando, FL, (1997) - In Printing
4. C. J. Janke, S. J. Havens, V. J. Lopata, and M. Chung; "Electron Curing of Epoxy Resins: Initiator and Concentration Effects on Curing Dose and Rheological Properties", 28th International SAMPE Technical Conference, Seattle, WA, 28, 901 (1996)
5. C. J. Janke; "Materials Development," Proc. 1st Electron Beam Curing of Composites Workshop, Oak Ridge, TN, Sept. 18-19, 1996
6. C. J. Janke, S. J. Havens, G. F. Dorsey, V. J. Lopata; "Toughened Epoxy Resins Cured by Electron Beam Radiation", 28th International SAMPE Technical Conference, Seattle, WA, 28, 877 (1996)
7. C. J. Janke, S. J. Havens, G. F. Dorsey, V. J. Lopata; "Electron Beam Curing of Epoxy Resins By Cationic Polymerization", 41st International SAMPE Symposium, Anaheim, CA, 41, 196 (1996)
8. L.T. Drzal, "Final Report: Adhesion of Carbon Fibers to Vinyl Ester Matrices", NSF State/Industry University Cooperative Research Center on Low-Cost, High-Speed Polymer Composite Processing, 1997
9. V. Bechel, C.J. Janke, M. Wilenski, G.P. Tandon, "Constituent Level Examination of an E-Beam Cured Graphite/Epoxy Composite", 46th International SAMPE Symposium 2001, May 6-10, 2001, Long Beach, CA, 46, 2115, (2001)
10. C.J. Janke, "Results on Improving the Toughness of E-Beam Curable Cationic Epoxy Resins", 2000 Electron Beam Curing Workshop, June 14-15, 2000, Oak Ridge, TN
11. C.J. Janke, "Status Report - Electron Beam Interface CRADA ", AFOSR E-Beam Panel Discussion, 47th International SAMPE Symposium 2002, May 12-16, 2002, Long Beach, CA, 47, (2002)
12. C.J. Janke, R.D. Lomax, S. Robitaille, S. Duggan, R.C. Serranzana, V.J. Lopata, "Improved Epoxy Resins Cured by Electron Beam Irradiation", 46th International SAMPE Symposium 2001, May 6-10, 2001, Long Beach, CA, 46, 2048 (2001)
13. B. J. Frame, G.E. Wrenn, and C.J. Janke, "Results of Electron Beam Prepreg Debulking Study", 47th International SAMPE Symposium 2002, May 12-16, 2002, Long Beach, CA, 47, (2002)

14. J. V. Crivello, M. Fan, and D. Bi, “The Electron-Beam Induced Cationic Polymerization of Epoxy Resins”, Applied Polymer Science, 44, 9 (1992)

15. J. V. Crivello, “UV and Electron Beam-Induced Cationic Polymerization”, Nuclear Instruments & Methods in Physics Research B, 151, 8 (1999)

16. M. Mascioni, J.M. Sands, G.R. Palmese, “Real time in-situ spectroscopic characterization of radiation induced cationic polymerization of glycidyl ethers” SAMPE International Symposium, 47,93 (2002)

17. M. Mascioni, J.M. Sands, G.R. Palmese, “Real time in-situ spectroscopic characterization of radiation induced cationic polymerization of glycidyl ethers”, *Nuclear Instruments and Methods in Physics Research B*, 208, 353-357, 2003

This page left blank intentionally.

APPENDIX A. PROJECT CONTACT DATABASE

This page left blank intentionally.

Appendix A. Project Contact Database

Organization	Name	Address	Phone/E-Mail
US Department of Energy	Dr. Terry Payne Laboratory Technology Research Program Manager	PO Box 2008 Bldg. 111UNV, MS 6499 Oak Ridge, TN 37831-6499	865 574 0008 Fax: 865 576 4181 pay@ornl.gov
Oak Ridge National Laboratory	Chris Janke* Senior Research Scientist	PO Box 2008 Bldg 5800, MS 6053 Bethel Valley Road Oak Ridge, TN 37831-6053	865 574 9247 Fax: 865 574 8257 jnk@ornl.gov
	Dr. Reza Dabestani	PO Box 2008 Bldg 4500S, MS 6100 Oak Ridge, TN 37831-6100	865 576 7325 Fax: 865 574 7596 dabestanir@ornl.gov
	Cliff Eberle Composite Materials Program Manager	PO Box 2008 Bldg 5800, MS 6053 Bethel Valley Road Oak Ridge, TN 37831-6053	865 574 0302 Fax: 865 574 8257 ecc@ornl.gov
	Jeanne Phillips Administrative Assistant	PO Box 2008 Bldg 5800, MS 6053 Bethel Valley Road Oak Ridge, TN 37831-60538	865 576 0382 Fax: 865 574 8257 zpi@ornl.gov
Air Force Research Laboratory	Dr. Vernon Bechel* Research Scientist	AFRL/MLBC 2941 P Street, Rm 136 Wright Patterson AFB, OH 45433-7750	937 255 9077 Fax: 937 656 4706 vernon.bechel@afrl.af.mil
	Janis M. Brown, Ph.D. Materials Research Engineer	AFRL/MLBD Bldg 654 2941 P Street Rm 136 WPAFB, OH 45433-7750	937 255 0968 Fax: 937 656 4706 janis.brown@wpafb.af.mil
Army Research Laboratory	Dr. James Sands* Research Fellow	ATTN: AMSRL-WM-MB Building 4600 Aberdeen Proving Ground, MD 21005	410 306 0878 Fax: 410 306 0759 jsands@arl.mil
NASA Langley	Harry Belvin*	MS 226 Hampton, VA 23681-0001	757 864 9436 Fax: 757 864 8312 h.l.belvin@larc.nasa.gov

Appendix A. Project Contact Database

Organization	Name	Address	Phone/E-Mail
	Dr. Tan Hou	MS 226 Hampton, VA 23681-0001	757-864-4251 Fax: 757 864 8312 t.hou@larc.nasa.gov
Acsion Industries	Vince Lopata* Director of Operations	PO Box 429 Pinawa MB R0E 1L0 Canada	204 753 2255 Fax: 204 753 8466 lopata@acsion.com
Adherent Technologies	Dr. Ron Allred* President	9621 Camino del Sol NE Albuquerque, NM 87111-1522	505 346 1685 Fax: 505 346 1686 rallred@adherent-tech.com
	Dr. Andrea Hoyt Polymer Projects Manager	11208 Cochiti SE Albuquerque, NM 87123	505 346 1688 Fax: 505 346 1687 aehoyt@adherent-tech.com
Applied Poleramic	Rich Moulton* President	850 Teal Drive Benicia, CA 94510	707 747 6738 Fax: 707 747 6774 poleramic@aol.com
Boeing	Dr. Mark Wilenski* Research Scientist	PO Box 3999 MS 73-09 Seattle, WA 98124-2499	425 237 0021 Fax: 425 234 2863 mark.wilenski@pss.boeing.com
Cytec Carbon Fibers	Hugh Player Product Development Manager	PO Box 849 Greeneville, SC 29602	864 299 9414 Fax: 864 299 9333 hugh_player@sc.cytec.com
E-BEAM Services	Dave Keenan* Midwest Operations Director	2775 Henkle Drive Lebanon, OH 45036	513 933 0031 x224 Fax: 513 933 0542 dkeenan@ebeamservices.com
Hexcel Corporation	Dr. Günther Jacobsen* Carbon Fiber Technology Manager	PO Box 18748 MS 2343L Salt Lake City, UT 84118-0748	801 508 8590 Fax: 801 508 8103 guenther.jacobsen@hexcel.com
	Rebecca Forsgren	PO Box 18748 Salt Lake City, UT 84118-0748	801 508 8137 Fax: 801 508 8103 Rebecca.Forsgren@hexcel.com

Appendix A. Project Contact Database

Organization	Name	Address	Phone/E-Mail
Lockheed Martin	Paige Kirn* Electron Beam Technologies Program Manager	1 Lockheed Blvd. (76108) PO Box 748 Bldg 501, Mail Zone 9383 Ft. Worth, TX 76101-0748	817 935 1763 Fax: 817 935 1369 paige.kirn@lmco.com
	Dr. Jin Choi	PO Box 29304, MS 4310 New Orleans, LA 70189-0304	504 257 1406 Fax: 504 257 1210 jinkyu.choi@maf.nasa.gov
STERIS Isomedix Services	Dr. Sergey Korenev* Director, Research Center for Radiation Physics	2500 Commerce Drive Libertyville, IL 60048	847 247 0970 Fax: 847 247 0882 Sergey_Korenev@steris.com
	Jerry Kriebel Manager Plant Operations	2500 Commerce Drive Libertyville, IL 60048	847 247 0970 Fax: 847 247 0882 jerry_kriebel@steris.com
UCB Chemicals Corporation	Morris A. Johnson* Senior Research Associate	2000 Lake Park Drive Smyrna GA 30080	770 801 3219 Fax: 770 801 3234 morris.johnson@ucb-group.com
	Dr. Sue Williamson Senior Research Scientist	2000 Lake Park Drive Smyrna, GA 30080	770 333 6990 Fax: 770 434 8314 sue.williamson@ucb-group.com
YLA	Susan Robitaille* Director of Research and Development	2970 C Bay Vista Court Benicia, CA 94510	707 747 2755 Fax: 707 747 2754 srobitaille@ylainc.com
	Tom Jonas R&D Business Development Manager	2970 C Bay Vista Court Benicia, CA 94510	707 747 2750 Fax: 707 747 6549 tjonas@ylainc.com
Michigan State University	Professor Lawrence T. Drzal* Director, Composite Materials and Structures Center	2100 Engineering Building East Lansing MI 48824-1226	517 353 5466 Fax: 517 432 1634 drzal@egr.msu.edu
	Dr. Mike Rich	2100 Engineering Building East Lansing MI 48824-1226	517 353 4696 Fax: 517 432 1634 rich@egr.msu.edu

Appendix A. Project Contact Database

Organization	Name	Address	Phone/E-Mail
National Research Council Canada	Dr. Kenneth Cole* Research Officer Industrial Materials Institute	75 de Mortagne Blvd Boucherville, Quebec J4B 6Y4 Canada	450 641 5144 Fax: 450 641 5105 kenneth.cole@nrc.ca
	Dr. Andrew Johnston Research Officer Institute for Aerospace Research	1500 Montreal Road Bldg. M-3 Ottawa, ON K1A 0R6 Canada	613 993 1159 Fax: 613 998 8609 Andrew.Johnston@nrc.ca

* Principal Investigator

APPENDIX B. EXIT CRITERIA FOR PERFORMANCE (PRE-PREG TAPE)

This page left blank intentionally.

Appendix B. Exit Criteria for Performance (Pre-preg Tape)

Level	Performance Criteria	Exit Supporting Data Type	Target Value
1	Thermal Performance	Wet Tg by DMA (DMA from –67F to 400F+)	290F, min; 375F target No change in E' from –67 to RT
1	Resin Toughness	K1c via Single Edge Notch Bend @ RT (ASTM D5045-93 SENB)	.82 ksi*√in min 1.6 ksi*√in target 3.2 ksi*√in (8551-7)
1	Resin Tensile Behavior	Neat resin tensile test @ RT	12 ksi min, 16 ksi target
1	Resin Weight	Resin Density	<= 1.4 g/cc
1	Quality laminates: Fiber Volume, Void Content, Resin Content	RC/FV/VV by Acid Digestion SEM of laminate cross-section	VV <= 0.5%, FV = 60+/-3%
1	Quality laminates: Resin is sticking to the fiber	SEM of a mechanical coupon after failure	Compare to SEM of thermals
1	Good Resin props and good fiber resin interaction	90 Flex OR Transverse Tension	9 ksi target for transverse tension
1	Good Intralaminar Shear	0 Short Beam Shear (SBS) Test @ RT	15 ksi min, 18 ksi target
1	Good Intralaminar Shear and compressive resin props	0 Flex (look for fiber tension failure before compressive resin failure)	TBD
2	Performance after exposed to jet fuel	0 SBS after jet fuel soak	95 % retention, min
2	Performance after exposed to solvents during assembly	0 SBS after IPA soak 0 SBS after Acetone soak	95 % retention, min
2	Performance after exposed to hydraulic fluid	0 SBS after hydraulic fluid soak	95 % retention, min
2	Tension Performance (typically fiber dominated)	0 Tension @ RTA, HW (Strength/Modulus ksi/msi)	IM7: 375/23(RTA), 340/21 (HW) AS4: 315/20.5(RTA), 280/20 (HW)
2	Compression Performance (resin and some fiber dominated)	0 Compression @ RTA, HW (Strength/Modulus ksi/msi)	IM7: 255/22(RTA), 185/18 (HW) AS4: 230/21(RTA), 175/18 (HW)
2	In-plane shear Performance (resin-fiber inter action)	IPS (+/- 45) Tension @ RTA, HW (Strength/Modulus ksi/msi)	IM7: 16/.8 (RTA), 13/.5 (HW) AS4: 13/.8 (RTA), 11/.5 (HW)
2	Robustness with holes (required for typical assemblies)	(OHC) Open Hole Compression (QI lay-up) @ RTA,HW Compression (QI lay-up) @ RTA	70% retention

Appendix B. Post CRADA Structural Material Tests

Level	**Performance Criteria**	**Supporting Data Type***	***Target Value***
3 (may be a 2)	Good out-of-plane behavior – needed at part edges, edges at bolt-holes, cut-outs etc. (poisson's through-the-thickness effect…ν_{12}, ν_{23} effect)	Edge Delamination Strength (EDS) [+/-25,90]s; get onset and failure stress at RT	
3 (may be a 2)	Good tensile behavior with holes – worst case is filled hole due to (in-plane) poisson's effect	Filled Hole Tension (FHT) Open Hole Tension (OHT)	
3		Un-notched Tension (UNT) at –67F (Cold Dry)	
3 (may be a 2)	Good performance if damaged; damage resistant	Compression Strength After Impact (CSAI) (most common damage seems to be 1500 in-lb/in) @ RT, HW	
3	Good bearing performance	Bearing Test (quasi laminate) @ RT, HW	

CRADA Exit Criteria for Processing (Pre-pregs)

Level	Processing Criteria	Exit Supporting Data Type*	*Target Value*
1	Debulking Temp and sensitivity (if any) to elevated temp prior to cure	Viscosity vs. Temp Viscosity at debulk temp vs. time	<=160F debulk
1	Resistant to Hazardous Exotherming	DSC of uncured (end-users need to know what NOT to do with uncured materials) Temp profile as a function of cure parameters	No hazardous exotherming
1	No hazardous by-products – do not exceed normal shop protection req'ts (latex gloves, little or minimal use of respirator)	TBD	TBD
1	Processing: resistance to creating in-situ porosity	Volatile content of resin	<= 1%
1	Processing: Out time – exposing pre-preg to normal light and humidity (65%RH, 75F)	SBS as a function of pre-preg moisture exposure SBS as a function of light exposure	95% retent 16 hours
1	Processing: Cure profile; Process Window	Properties (DMA, SBS) as a function of cure profiles	
1	Availability	Supplier chain list	Na
2	Shelf Life	TBD: Accelerated Age Testing (SBS) Note: Save material at end of CRADA for real time age evaluation (SBS)	3 years @ RT
2	Quality: Good Wet-out	Discussed in April '00 M&P telecon	Qualitative
2	Quality: Good Tack	TBD (vertical stick type test)	Qualitative
2	Quality: Good Drape	TBD	Qualitative
2	Capability to B-stage	DMA as a function of delivered dose Visual appearance as a function of dose	B-stageable is desirable

*Again, there may be data that leads to the exit data. This is a preliminary list and feedback is welcome.

This page left blank intentionally.

APPENDIX C. IRRADIATOR PARAMETERS

This page left blank intentionally.

Appendix C. Irradiator Parameters

Company / Designation	Acsion *I10/1*	Acsion *Gammacell 220*	Isomedix *Rhodotron TT200*	EB Services *CBS*	EB Services *CBN*	Boeing *BREL Linac*	Boeing *Gammacell 220*	Boeing *Shepard Cell*	Notre Dame *Linac*
Accelerator Parameters									
Voltage, MeV (max.)	9.7	1.8	5	4.5	10	10	1.8		8
Voltage, MeV (min.)				2.5		5			
Power, kW (max.)	0.75		80	150	50	1			
Power, kW (min.)			0		10	0.01			
Beam current, mA (max.)	0.077		16	33.3	5.0	0.1			
Beam current, mA (min.)	0								
Pulse current, mA(max.)	64		16	33.3	89	333			4000
Pulse current, mA(min)	64				89				
Rf frequency, GHz	3		0.1075	DC	1.3	3			
Pulse length, us (max.)	4				200	10			1.5
Pulse length, us (min.)					40	0.004			0.002
Pulse repetition rate (max), Hz	300		CW	DC	280	30			
Pulse repetition rate (min), Hz	0				250	0			
Scan rate, Hz	2		200	100	6	0.33			
Beam Parameters									
Beam delivery direction	vertical		horizontal	vertical	vertical	vertical			
Width per scan, metres (max.)	0.6		1	1.73	0.41	0.61			
Width per scan, metres (min.)	0.1		0.3	0.1	0.79	0.1			
Height from window, cm	60			127	127				
Beam diameter, cm (50%)[1]	9								
Beam diameter, cm (10%)[1]	14		14	14	14	14			
Conveyor Belt Parameters									
Height from window, cm	60		25	127	127				
Maximum width, cm	60		126	173	80	30			
Minimum width, cm	5		36	10	10				
Maximum speed, cm/s	13		25.4	24	2	0.830			
Minimum speed, cm/s	0.05		2.54	2.54	0.04	0			
Reversible (Y or N)	Y			N	N	Y			

[1] In beam diameter specification, specified percentage of beam current is contained within specified beam diameter at a specified distance from vacuum window

Appendix C. Irradiator Parameters

Company / Designation	Acsion *I10/1*	Acsion *Gammacell 220*	Isomedix *Rhodotron TT200*	EB Services *CBS*	EB Services *CBN*	Boeing *BREL Linac*	Boeing *Gammacell 220*	Boeing *Shepard Cell*	Notre Dame *Linac*
Return time				3 - 6 min	17 min				
Part Size									
Width, metres	4	0.152		140	140	0.91	0.152	0.25	
Length, metres	3			179	366	1.52		1.02	
Height, cm	100	0.203		127	127		0.203	0.25	
Weight, maximum	700			750	1500				
Radiation Parameters									
Instantaneous dose rate, MGy/s (max.)[2]	19	55 Gy/min	5	10	26	98	105 Gy/min	60 Gy/min	
Instantaneous dose rate, MGy/s (min.)[3]	0.53		0.13	0.27	0.73	2.73			
Areal dose rate, kGy-cm^2/s(max)	108		22400	46667	7000	140			
Support Equipment/Facilities									
Vacuum equipment	yes			no	no	yes			
Air lines	yes			yes	yes	yes			
Preparation Lab	yes			no	no	yes			
X-ray conversion equipment	yes			no	no	yes			
thermocouples	yes					yes			
Humidity measurement	yes					yes			
Dosimetry	FW3, Gaff								

[2] 10 cm from beam exit
[3] 60 cm from beam exit

APPENDIX D. STANDARD IRRADIATION LOG SHEET

This page left blank intentionally.

Appendix D. Standard Irradiation Log Sheet

Date:	**Time:**	**Recorded by:**

Radiation Parameters	
Logged Variables	
Beam energy	MeV
Beam current	mA
Pulse duration	sec
Pulse frequency	Hz
Scan width (at conveyor)	cm
Scan frequency	Hz
Conveyor speed	cm/s
No. of passes	
Rest period	sec
Dose increment (logged)	kGy/pass

Machine Parameters	
Conveyor height	cm
Scan horn height	cm
X-ray converter height	cm
Beam spot diameter (at conveyor)	cm

Calculated Data	
Total dose	kGy
Dose increment (calc)	kGy/pass
Beam power	kW
Pulse current	mA
Multi-pass dose rate	kGy/sec
Single-pass dose rate	kGy/sec
Instantaneous dose rate	kGy/sec
Max. pt. Inst. dose rate	kGy/sec
Beam duty factor	
Pass duration	sec
Beam spot dia (on target)	cm
Scan width (on target)	cm

Notes:

Ambient Conditions	
Temperature	Celsius
Relative humidity	%
Barometer	mm Hg
Measurement location:	

Target Data		
Description:		
Part dwg/spec ID		
Cure setup picture filename		
Length		cm
Height		cm
Width		cm
Irradiation height		cm
Specified cure temperature	RT	Celsius
Part temperature recorded?		
Temp sensor type		
Temp sensor location(s)		
Temp record filename		
Vacuum bagged?		
Vac during cure?		

Calibration Data		
Radiation type	Electron	
Dose increment		kGy/pass
Conveyor speed		cm/s
Scan width (at conveyor)		cm
Irradiation height		cm
Beam current		mA
Pulse current		mA
Pulse duration		sec
Gaussian peak (at conveyor)		kGy/pulse
Gaussian peak (at conveyor)		kGy/sec

This page left blank intentionally.

APPENDIX E. GLOSSARY OF STANDARD TERMS

This page left blank intentionally.

Glossary of irradiation terms

Note: *For DC and CW accelerators, the terms "pulse" and "pulse period" in all definitions can be replaced by "a time period on the order of a microsecond".*

Note*: Definitions assume a vertical beam.*

General definitions

- Beam current, delivered beam current, time-averaged beam current (A)
  Current carried by electrons in the beam at the scan horn exit. Constant in CW and DC accelerators. Integrated over a time period that is a positive integer multiple of the pulse period in pulsed accelerators.

- Beam duty factor, duty factor (0 to 1, dimensionless)
  The fraction of time during which the machine is actually emitting electrons. 1 for CW and DC accelerators. For pulsed accelerators, the pulse duration divided by the pulse period.

- Beam energy (MeV)
  Nominal energy of electrons at the accelerator exit.

- Beam height (cm)
  Distance between the scan horn exit (vacuum window) and the irradiated surface.

- Beam length (cm)
  Length of the beam as seen by a target moving along the conveyor. Beam length is normally equal to beam spot diameter.

- Beam power, delivered beam power (Watts or kW)
  Power delivered by the beam at the scan horn exit, integrated over a time period that is a positive integer multiple of the pulse period in pulsed accelerators. Beam power is the product of beam current and beam energy.

- Beam spot
  The area that is irradiated, or "illuminated", by the beam, at any given time. The edge of the beam spot is defined by the "iso-dose rate" line where dose rate is reduced to 10% of the peak dose rate at the center of the beam spot.

- Continuous wave (CW) accelerator
  RF accelerator with constant beam current.

- Conveyor height (cm)
  Distance between the scan horn exit (vacuum window) and the conveyor surface, when the scan horn is vertically oriented..

- Conveyor speed (cm/s)
  Speed at which the irradiation target is moved, by the conveyor, through the beam.

- Current density (A/cm^2)
  Current per unit area

-

Appendix E. Glossary of Standard Terms

- Direct current (DC) accelerator
  Accelerator in which current is constant and electrons are electrostatically accelerated.

- Height, part height, target height (cm)
  Part dimension measured vertically.

- Illumination period, dwell period
  The time period during which a specified point is being consistently irradiated. That is, the time required for a specified point in the irradiation target to pass through the beam length.

- Irradiated surface
  The surface where the beam enters the irradiation target

- Irradiation height (cm)
  Distance between the conveyor surface and irradiated surface. Also conveyor height minus beam height.

- Irradiation target, target, part
  The item being irradiated.

- Length (cm)
  Part dimension measured along the axis of conveyor motion.

- Pass
  Translation of the irradiation target, through the beam length, one time.

- Pulsed accelerator
  An accelerator, usually RF type, in which the beam current is delivered in discrete pulses.

- Radio frequency (RF) accelerator
  Accelerator in which RF energy is used to power the accelerating structure and provide the accelerating voltage.

- Rest period
  The time period between irradiations for a specified point in the irradiation target. That is, the amount of time that a specified point remains unexposed to the scanned beam, between passes through the beam

- Scan height (cm)
  Distance between the irradiated surface and scanning apex. Also the sum of scan horn height and beam height.

- Scan horn height (cm)
  Distance between the vacuum window and scanning apex, i.e., height of the triangle tended by beam scan limits (sides of triangle) and vacuum window (bottom of triangle).

- Scan width (cm)
  Width of the beam scan, measured at the conveyor, between centers of the extreme spot locations.

- Width (cm)
  Part dimension measured horizontally transverse to the axis of conveyor motion.

- X-ray converter
  A metal target that is inserted into the electron beam path to produce x-rays.

- X-ray converter height (cm)
  Distance between the conveyor belt and the x-ray converter.

Dose, Dose increment, & Dose rate definitions

- Absorbed dose (kGy)
  Amount of radiation energy absorbed per unit mass of irradiated material. 1 kGy = 1 kJ/kg.

- Dose (kGy)
  Energy per unit mass. Although not strictly correct, the terms “dose” and “absorbed dose” are used interchangeably.

- Dose increment, dose per pass (kGy)
  The dose delivered to a target during a single pass through the beam.

- Dose profile, beam profile, spot profile (dimensionless).
  Spatial dose distribution in the beam spot, normally represented by a Gaussian function.

- Dose rate (kGy/s)
  1. The rate of dose delivery during a specified time period.
  2. The dose, integrated over an integer multiple of pulse periods, and averaged over the scanned area on a stationary target, divided by the time period of dose measurement.

- Instantaneous dose rate, area-averaged instantaneous dose rate (kGy/s)
  The dose rate during the pulse, area averaged over the beam spot.

- Multi-pass dose rate, average dose rate (kGy)
  The dose rate, area-averaged over a target during a period comprising multiple passes through the beam; equals total dose delivered to the part, divided by total time elapsed between commencement and completion of part irradiation.

- Pass period (s), pass duration
  The time required for a target to complete one pass through the beam.

- Point dose rate, local dose rate (kGy/s)
  The dose rate, as experienced at a specified point in the irradiation target, and integrated over a specified time period.

- Point instantaneous dose rate, local instantaneous dose rate (kGy/s)
  The dose rate, as experienced at a defined point in the irradiation target, and measured during a specified pulse (the value normally changes from pulse to pulse because of beam scanning and the dose profile).

- Single-pass dose rate (kGy/s)
  The dose rate area-averaged over a target during a single pass through the beam; equals dose increment divided by the pass period.

- Surface dose (kGy)
  The dose measured by dosimeter(s) affixed to the surface of an irradiation target. This is generally assumed (the assumption introduces a negligible error) to be the dose that is absorbed by the irradiation target at the surface where the respective dosimeter is affixed.

Pulse parameter definitions

Note: Some of the definitions are illustrated at the end of this appendix.

- Pulse, macro-pulse
  In certain accelerators, usually RF linacs, the time period when current is flowing. In pulsed machines, electrons are generated in short pulses, separated by longer periods with null current. Typically the pulses are order microseconds in duration, and the time between pulses is order milliseconds.

- Pulse charge, pulse area (C)
  Charge delivered during a pulse.
  Pulse charge = pulse current x pulse duration. Graphically, for a rectangular pulse, it is pulse width x pulse height (hence pulse area).

- Pulse current, pulse height, instantaneous beam current (A)
  Current carried by electrons in the beam, during a pulse.

- Pulse duration, pulse width, pulse length (s)
  The time between the beginning and end of an electron pulse in a pulsed accelerator. This is technically measured at full width half maximum, however pulses are typically highly rectangular. Pulse duration is normally order μs for industrial accelerators and ns for pulse radiolysis accelerators.

- Pulse frequency, repetition rate, rep rate (Hz)
  The number of pulses per second in a pulsed accelerator. Reciprocal of pulse period.

- Pulse period (s)
  Time between the same point (e.g., beginning) of consecutive pulses. Reciprocal of pulse frequency.

RF parameter definitions

Note: See RF parameter illustration below. Illustration is for a pulsed RF accelerator, however RF definitions are also valid for a CW RF accelerator.

- Bucket, micro-pulse, mini-pulse
  Term applying to RF accelerators. Refers to the fact that electrons arrive in tiny bunches, like surfers riding waves, with the wave period being the reciprocal of RF frequency. Each wave delivers a "bucket" of electrons. Ref. appended illustrations.

- Bucket height, bucket current, RF pulse current (A)
  Current carried by electrons in the beam during an RF pulse. Measured on the time scale of the RF driving frequency.

- Bucket width (s)
  The width of a bucket, measured at Full Width Half Maximum.

- RF frequency, bucket frequency (Hz)
  The RF frequency, *and* the frequency with which buckets arrive, in an RF accelerator. Usually 1 – 10 GHz.

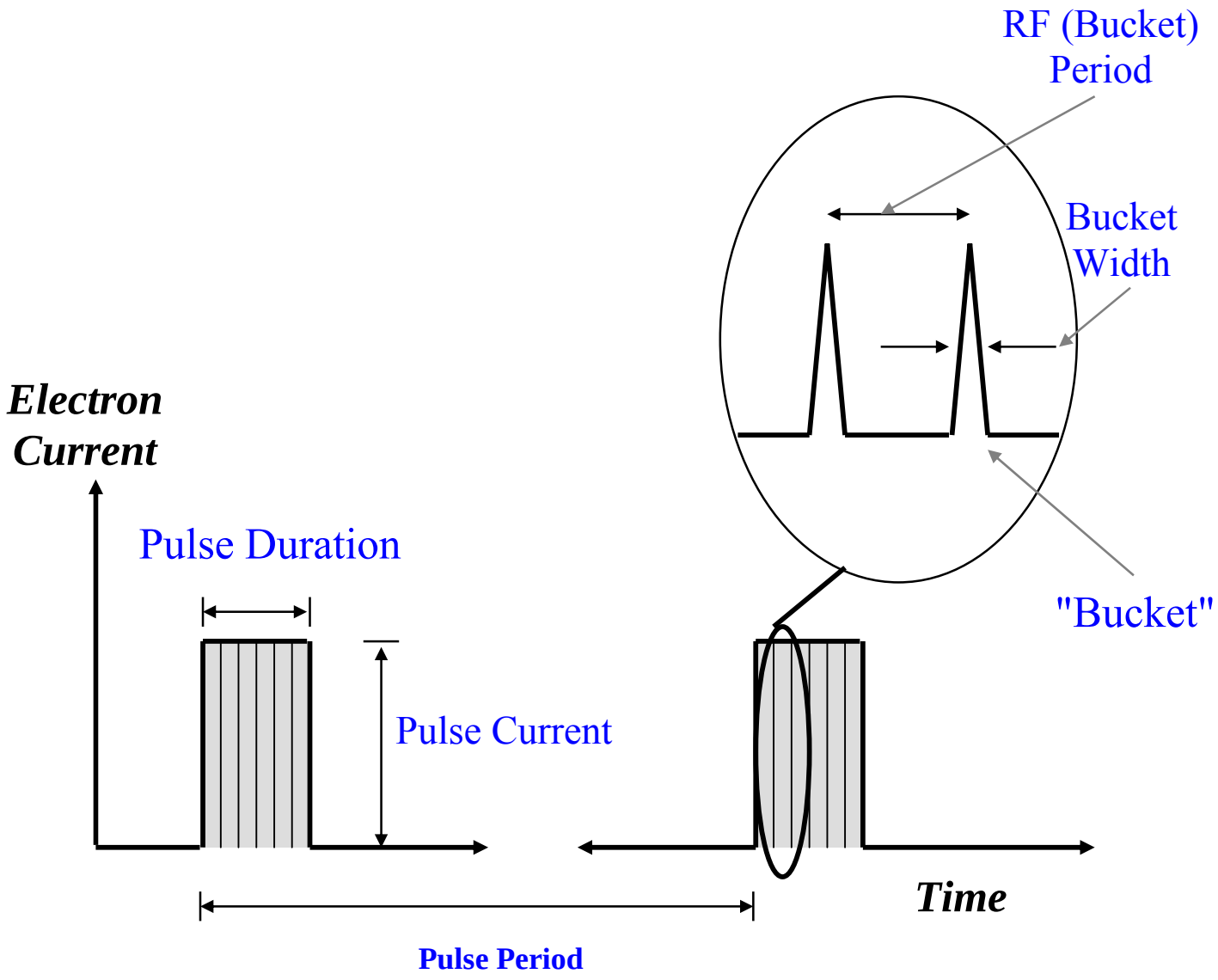

Figure E-1. Illustration of some pulse and RF parameter definitions.

DISTRIBUTION

Internal

1. E. E. Bloom
2. C. C. Eberle
3. R. Dabestani
4. E. T. Grostick
5. C. J. Janke
6. R. E. Norris
7. T. L. Payne
8. P. S. Sklad
9. C. D. Warren
10. DOE-WFO
11. ORNL Site Office
12-13. ORNL Central Research Library
14. Office of Technical Information and Classification

External

15. R. Allred, Adherent Technologies, 9621 Camino del Sol NE, Albuquerque NM 87111-1522
16. S. J. Barish, DOE, SC-55/Germantown Bldg, 1000 Independence Ave SW, Washington DC 20585-1290
17. V. Bechel, USAF Research Laboratory, AFRL/MLBD, 2941 P St, WPAFB OH 45433-7750
18. L. T. Drzal, Michigan State University, 2100 Engineering Bldg, East Lansing MI 48824-1226
19. M. Grant, Acsion Industries, PO Box 429, Pinawa MB R0E 1L0 Canada
20. T. Hou, NASA Langley Research Center, MS 226, Hampton VA 23681-0001
21. G. Jacobsen, Hexcel Fibers, PO Box 18748, Salt Lake City UT 84118-0748
22. A. Johnston, NRC Canada, 1500 Montreal Rd Bldg M3, Ottawa ON K1A 0R6 Canada
23. D. Keenan, E-Beam Services, 2775 Henkle Dr, Lebanon OH 45036
24. P. Kirn, Lockheed Martin, 1 Lockheed Blvd, ATTN: Paige Kirn, Mail Zone 5954, Ft. Worth TX 76108
25. S. Korenev, STERIS Isomedix Services, 2500 Commerce Drive, Libertyville, IL 60048
26. R. Moulton, Applied Poleramic Inc., 850 Teal Dr, Benicia CA 94510
27. H. Player, Cytec Carbon Fibers, PO Box 849, Greeneville SC 29602
28. S. Robitaille, YLA Inc., 2970 C Bay Vista Court, Benicia CA 94510
29. J. Sands, US Army Research Laboratory, AMSRL-WM-MB, Bldg 4600, Aberdeen Proving Ground MD 21005
30. M. S. Wilenski, Boeing, PO Box 3999, MS 73-09, Seattle WA 98124-2499
31. S. Williamson, UCB Chemicals Corporation, 2000 Lake Park Drive, Smyrna, GA 3008